Cerebral ischemia induced proteomic alterations: consequences for the synapse and organelles

Costain, Willard J.; Haqqani, Arsalan S.; Rasquinha, Ingrid; Giguere, Marie-Soleil; Slinn, Jacqueline

Publisher's version / Version de l'éditeur:
https://doi.org/10.5772/32035
Advances in the Preclinical Study of Ischemic Stroke, pp. 85-116, 2012-03-16

5

Cerebral Ischemia Induced Proteomic Alterations: Consequences for the Synapse and Organelles

Willard J. Costain[1], Arsalan S. Haqqani[2], Ingrid Rasquinha[1], Marie-Soleil Giguere[2] and Jacqueline Slinn[3]
[1]*Glycosyltransferases and Neuroglycomics, Institute for Biological Sciences, National Research Council, Ottawa, ON,*
[2]*Proteomics, Institute for Biological Sciences, National Research Council, Ottawa, ON,*
[3]*Cerebrovascular Research, Institute for Biological Sciences, National Research Council, Ottawa, ON,*
Canada

1. Introduction

The synapse is the focal point for neuronal communication and neuron-glia interactions. Synaptic structure and function are intimately related and many of the proteins that provide structure to the synapse also regulate synaptic function (Abe et al. 2004, Couchman 2003, Ehlers 2002, Passafaro et al. 2003). The synaptic structure - function relationship is highly apparent during pathological conditions. This is exemplified in neurodegenerative disorders, such as Alzheimer's disease, where synaptic function is positively correlated with neuronal function (Gasic & Nicotera 2003) and viability (Deisseroth et al. 2003), with synaptic pathology preceding cell death (Gasic & Nicotera 2003).

Maintenance of synaptic structure and functionality is a process that is highly energy dependent. Studies of synaptosomal morphology and metabolism have indicated that the synapse is highly susceptible to ischemic damage (Pastuszko et al. 1982, Rafalowska et al. 1980, Sulkowski et al. 2002, Enright et al. 2007, Zhang & Murphy 2007). This exceptional requirement for energy necessitates the localization of numerous mitochondria proximal to the synaptic bouton and mitochondria are a commonly observed feature in synaptosomal preparations (Costain et al. 2008). Synaptosomal metabolic activity (Rafalowska et al. 1980) and the rate of neurotransmitter re-uptake (Pastuszko et al. 1982) are decreased following acute hypoxia. Furthermore, Sulkowski *et al* (2002) observed that ischemia decreases synaptosomal oxygen consumption and metabolic capacity for a period of 24 hours.

Cerebral ischemia induces a marked depletion in synaptic vesicle content and increases the number of damaged mitochondria (Sulkowski et al. 2002, Costain et al. 2008). Importantly, ischemia-induced alterations in synaptosomal morphology are indistinguishable from that of brain slices (Sulkowski et al. 2002). Ischemia-like conditions (hypoxic stress or excitotoxicity) induce dramatic and rapidly reversible structural/morphological changes in dendritic spines (Hasbani et al. 2001, Mattson et al. 1998, Park et al. 1996, Enright et al. 2007,

Zhang & Murphy 2007). The structural (Park et al. 1996) and biochemical alterations (Martone et al. 1999) at the synapse rapidly return to normal following cessation of ischemic stressors. This initial period of apparent recovery is followed by a period of morphological and biochemical alterations that persist for upwards of 24 hours (Martone et al. 1999). Similarly, dysregulation of synaptic adhesion is observed prior to the onset of neuronal cell death and continues thereafter (Costain et al. 2008). These studies indicate that the synapse is highly responsive to ischemia and is an important modulator of post-ischemic neuronal fate. Signals triggered at the synapse propagate toward the cell body and instigate delayed post-ischemic neuronal death in a process termed as ***synaptic apoptosis*** (Mattson et al. 1998).

Synaptically localized signals, either anti- or pro-apoptotic, can be propagated to the cell body in both an anterograde and retrograde manner (Mattson & Duan 1999). Apoptotic stimuli have been shown to induce caspase-3 activation, mitochondrial membrane depolarization and phospholipid asymmetry in isolated synaptosomes (Mattson et al. 1998). Similarly, trophic factor withdrawal increases axonal caspase-3 activity, but not within the neuronal soma (Mattson & Duan 1999). In hippocampal neurons, apoptotic signals initiated at the dendrites have been shown to subsequently spread toward the cell body (Mattson & Duan 1999). Synaptic apoptosis may be a mechanism that is necessary for synaptic remodeling under non-pathological conditions as well as contributing to or initiating neuronal apoptosis during pathological conditions. Pro-apoptotic proteins have been found to play a role in non-pathological processes such as neurogenesis, neurite outgrowth and synaptic plasticity (Mattson & Gleichmann 2005). This suggests that signals triggered at the synapse may propagate toward the cell body and instigate post-ischemic neuronal death.

Cellular protein levels are determined by the balance between the rates of synthesis and degradation, and cerebral ischemia has a pronounced effect on these processes. The transcriptional response to cerebral ischemia has been studied using high throughput methods under a variety of experimental conditions (Gilbert et al. 2003, MacManus et al. 2004). Similarly, cerebral ischemia-induced protein degradation has been examined for a variety of individual proteins. Activation of a variety of proteases, such as members of the caspase, calpain and cathepsin families, is a well-described consequence of cerebral ischemia (Vanderklish & Bahr 2000, Kagedal et al. 2001). Complicating this is the observation that cerebral ischemia causes proteosomal (DeGracia et al. 2002), lysosomal (Costain et al. 2010), mitochondrial (Costain et al. 2010) and endoplasmic reticulum dysfunction (Ge et al. 2007). Thus, it is almost impossible to predict post-ischemic cellular protein levels from gene expression data alone. When focusing on a subcellular structure, such as the synapse, an additional mechanism will impact protein levels. Intracellular transport mechanisms can target a protein to a specific region or be involved in sequestering proteins away from their original location (Zhao et al. 2005, Vanderklish & Bahr 2000). As a result of these factors, the best approach for determining post-ischemic synaptic protein levels is to perform a direct assessment using proteomic methodologies.

An understanding of the cell death processes that are precipitated by exposure to cerebral ischemia is necessary for designing rational therapeutic intervention. Considering that cell death can be mediated by multiple inter-related mechanisms, it is perhaps unsurprising that the majority of single target small molecules have failed in clinical trials for stroke (Ginsberg 2008). The role of apoptotic cell death in cerebral ischemia has long been studied (Hou &

MacManus 2002), and more recently ischemia induced autophagy has become an active area of interest (Liu et al. 2010). While necrotic cell death is well known to occur in cerebral infarcts, the recent identification of programed necrosis, or 'necroptosis', has reinvigorated research in ischemia-induced necrotic cell death.

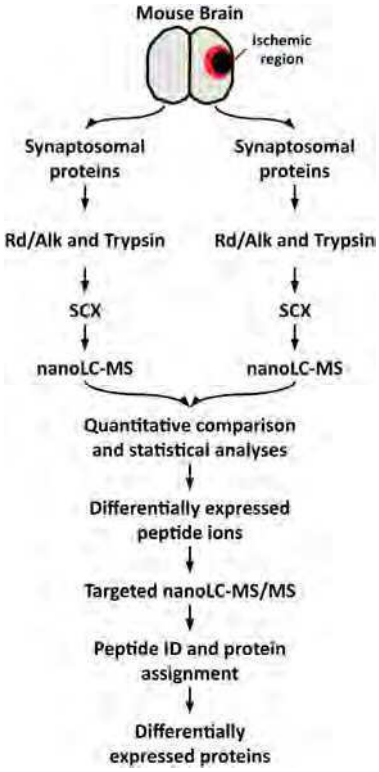

Fig. 1. Outline of the ischemic synaptosomal proteomic analysis procedure. Focal ischemia was performed 20 hours prior to the isolation of the ipsilateral (ischemic) and contralateral (non-ischemic) mouse brain hemispheres. Synaptosomes were isolated from the entire forebrain hemispheres and processed as described in the diagram.

While cell death mechanisms are typically viewed as pathways involving multiple proteins and organelles, neuronal pathology can also be examined from an organelle centric perspective. Organelle dysfunction can precipitate the initiation of cell death pathways, rather than simply being relay points for signaling events. The essence of this distinction is the difference between extrinsic activation of cell death and internal/intrinsic activation. The primary route of activation of cell death following cerebral ischemia is through intrinsic pathways involving the mitochondria, lysosomes endoplasmic reticulum, and nucleus (Yamashima & Oikawa 2009, Chen et al. 2010, Ankarcrona et al. 1995). Thus, a strategy that involves examining the interaction between organelles during pathological conditions may enable the identification of new targets that can be exploited as therapies for cerebral ischemia.

The effects of cerebral ischemia are often, by necessity, described from a highly reductionist point of view, with most studies focusing on specific signaling pathways or individual molecules. Conversely, genomic and proteomic datasets offer the opportunity to expand the scope of understanding and enable the interpretation of systematic responses. While there is a wealth of data available describing neuronal proteins localized in synaptosomes as well as pre-synaptic and post-synaptic preparations, to date studies on the effects of cerebral ischemia on the synaptic proteome are limited (Costain et al. 2008). The aim of this chapter is to integrate new and existing genomic and proteomic datasets to provide a comprehensive understanding of the effect of cerebral ischemia on the function of neuronal organelles, as well as their role in mediating cell death and / or neuroprotection.

2. Materials and methods

2.1 Animal care

A local committee for the Canadian Council on Animal Care approved all procedures using mice. The C57B mice were purchased from Charles River Canada (St-Constant, PQ). Under temporary isoflurane anesthesia, the mice (20-23 g) were subjected to occlusion of the left middle cerebral artery (MCAO) using an intraluminal filament as previously described (Costain et al. 2008). After 1 hr of ischemia, the animals were briefly reanesthetized, the filament withdrawn and wounds sutured. After 20 hrs of reperfusion, mice were briefly anesthetized with isoflurane and the brain rapidly excised and dissected on ice.

2.2 Synaptosome preparation

Contralateral (CT) and ischemic (IS) hemispheres from one mouse were manually homogenized in 2 ml of HM buffer (0.32 M sucrose, 1 mM EDTA, 0.25 mM DTT, 1 U/ml RNasin (Promega)) using a dounce homogenizer, 800 rpm 13 strokes at 4 °C. The homogenates were centrifuged (1000 g for 10 min at 4 °C) and the supernatant retained. The pellet was homogenized and centrifuged (as before) a second time. The first and second supernatants were transferred to 2 ml polycarbonate tubes and centrifuged at 20,000 g for 20 min at 4 °C. The resultant pellet was resuspended in 2 ml HM buffer using a dounce homogenizer. Discontinuous sucrose:percoll gradients were prepared by layering 2 ml each, in order, of 25% (percoll in HM buffer), 15%, 10% and 3% into 10 ml polycarbonate centrifuge tubes. One ml of the sample was then layered on top of a gradient and centrifuged at 32,000 g for 5 min at 4 °C. Five fractions were collected following centrifugation: F1 - 3% percoll (cytoplasm), F2 - interface between 3% and 10% percoll (myelin), F3 - interface between 10% and 15% percoll (small synaptosomes, myelin & mitochondria), F4 - interphase between 15% and 25% percoll (intact synaptosomes), and F5 - pellet (mitochondria). Fractions F1 - F4 were made up to 3 ml with HM buffer and centrifuged at 12,000 g for 20 min at 4 °C. The supernatant was removed and the pellet washed with 1 x PBS, twice (each time spinning at 12000 x g for 10min). The final pellet was resuspended in either HM buffer or 50 mM Tris pH 8.5, 0.1% SDS. The physical and biochemical characteristics of the synaptosome preparation used here are described in further detail in Costain *et al*. (2008).

2.3 Protein preparation, digestion and ion exchange chromatography

Proteins from each synaptosome sample were precipitated by adding 10 volumes of cold acetone and incubating at 1 h at -20 °C followed by centrifugation at 5000×g for 5 min. Pellets

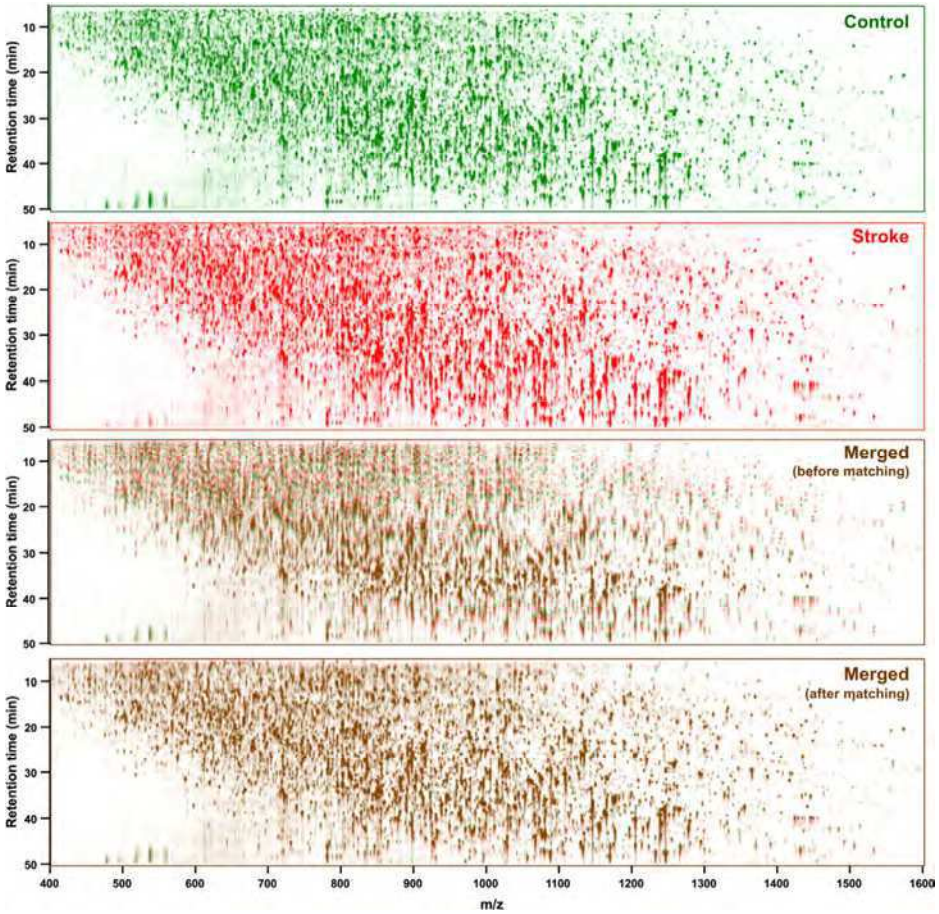

Fig. 2. NanoLC-MS analysis of contralateral (control) and ipsilateral (stroke) samples. Shown are images representing the nanoLC-MS data from each sample, where each spot represents a peptide ion. MatchRx software was used to extract peptide data, align the control and stroke datasets and correct retention time variations. Shown are the merged images before and after MatchRx-dependent correction. More than 5000 ions were detected per sample.

were dissolved in an appropriate volume of denaturing buffer (50 mM Tris-HCl, pH 8.5, 0.1% SDS) to a final protein concentration of 2 mg/mL. One hundred µg of each protein was transferred to a fresh tube. The proteins were reduced using dithiothrietol (4 mM, 10 min at 95 °C), alkylated using iodoacetamide (10 mM, 20 min at room temperature in dark), and digested using 5 µg of MS-grade trypsin gold (Promega, 12-18 h at 37 °C). The digested peptides were diluted 10-fold in 10 mM KH_2PO_4, pH 3.0, 25% acetonitrile and loaded onto a cation exchange column (POROS® 50 HS, 50-µm particle size, 4.0 mm x 15 mm, Applied Biosystems) for separation. Five fractions were eluted using step-gradient of 0-350 mM KCl. Each fraction was evaporated to dryness and dissolved in 5% acetronitrile, 1% acetic acid for analysis by mass spectrometry (MS).

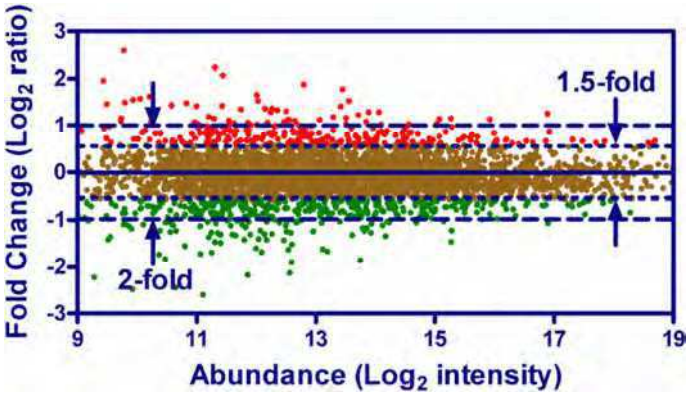

Fig. 3. Scatter plot showing relative expression of peptides in stroke and control synaptosomes. Peptide intensities were extracted from nanoLC-MS runs using MatchRx and ratio-intensity plots of stroke-vs-control samples after global median normalization were plotted. Peptides showing up (red) or down (green) regulation by 1.5-fold in stroke relative to control samples and showing a p <0.05 were considered differentially expressed. These corresponded to ~27% of the peptides and were used for targeted identification using nanoLC-MS/MS.

2.4 MS analysis and protein identification

A hybrid quadrupole time-of-flight MS (Q-TOF Ultima, Waters, Millford, MA) with an electrospray ionization source (ESI) and with an online reverse-phase nanoflow liquid chromatography column (nanoLC, 0.075 mm × 150 mm PepMap C18 capillary column, Dionex/LC-Packings, San Francisco, CA) was used for all analyses. Samples were separated on the nanoLC column using a gradient of 5-75% acetonitrile and 0.2% formic acid in 90 min, at 350 nL/min supplied by a CapLC HPLC pump (Waters). Five percent of each sample was first analyzed by nanoLC-MS in a survey (MS-only) mode for quantitation using MatchRx software as described recently (Haqqani et al. 2008). Briefly, each scan was background-subtracted, Savitzky-Golay-based smoothed, and centroided using Masslynx software v4.0 (Waters) and exported as an mzXML file (Pedrioli et al. 2004). Using MatchRx software, isotopic distribution pattern, charge state, and quantitative abundance of peptides in each nanoLC-MS run were determined. The peptides were then aligned across multiple nanoLC-MS runs through a neighboring-peak finding algorithm (Haqqani et al. 2008) followed by quantitatively comparing the levels of each peptide in the ipsilateral and contralateral fractions to identify differentially expressed peptides. Peptides showing consistent $\log_2$ fold-change of >1.5 or <-1.5 among biological replicates and showing significant difference from mean expression levels (p < 0.05, Wilcoxon matched pairs test) were considered differentially expressed. Images of each run were also generated to visually validate the differentially expressed peptides using MatchRx (**Fig. 4**). To sequence the differentially expressed peptides, they were included in a 'include list'. Another 5% of each sample was then re-injected into the mass spectrometer, and only the peptides included in the 'include list' were sequenced in MS/MS mode (targeted nanoLC-MS/MS). All MS/MS spectra were obtained on 2+, 3+, and 4+ ions. Peak lists were submitted to a probability-based search engine, Mascot version 2.2.0 (Matrix Science Ltd., London, U.K.) (Hirosawa et

al. 1993). The initial database utilized was a composite of forward and reverse Uniprot-Swiss-Prot *Mus musculus* protein database (Aug 2011 containing 16,390 sequences). Unmatched peptides were subsequently searched against the remaining Uniprot-Swiss-Prot database (Aug 2011 containing 531,473 sequences). Searches were performed with a specified trypsin enzymatic cleavage with one possible missed cleavage. The false-positive rates (FPR) in database searching by Mascot were calculated as described earlier (Peng et al. 2003): FPR = (2 × Nrev)/(Nrev + Nfwd), where Nrev is the number of peptides identified (after filtering) from the reverse-database, and Nfwd is the number of peptides identified (after filtering) from the forward database. To maximize the number of peptides and keep the FPR < 0.5%, ion scores > 20, parent ion tolerance of < 0.1 Da, fragment ion tolerance of < 0.2 Da, and minimal number of missed cleavages were chosen. As an independent statistical measure of peptide identification, Peptide Prophet probabilities were also measured. All identified peptides had $p \geq 0.90$. The MS/MS spectrum of each differentially expressed peptide pair was manually examined and confirmed.

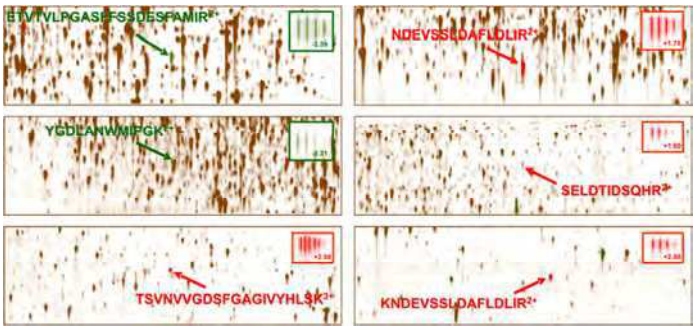

Fig. 4. Examples of differentially expressed proteins on nanoLC-MS images. Shown are merged images representing nanoLC-MS data of control (green image) and stroke (red image) samples. The two down-regulated peptides (green) are from 3-Oxoacid CoA Transferase 1 (Q9D0K2, Oxct1) and the four up-regulated peptides (red) are from glial high affinity glutamate transporter (P43006, Slc1a2). Peptides were identified by targeted nanoLC-MS/MS. In each image, *inset* shows a close-up image of the indicated peptide and the fold-change in stroke sample relative to control. For detailed list see **Tables 1** and **2**.

3. Results

3.1 Label-free proteomic analysis of ischemic synaptosomes

An outline of the experimental procedure is provided in **Fig. 1**. Following cerebral ischemia, the ipsilateral and contralateral hemispheres were separated and synaptosomal proteins isolated. The proteins from each sample were digested into sequenceable peptides, separated into 4 cation exchange chromatography fractions and analyzed by nanoLC-MS to quantify the level of each peptide. Each cation exchange fraction contained more than 12,000 peptide peaks as identified by nanoLC-MS analysis (**Fig. 2**). MatchRx software was thus used to identify quantitative differences in the nanoLC-MS runs between all the ipsilateral and contralateral fractions. The software extracts peptide-peak intensities and enables correction of retention time variations amongst multiple nanoLC-MS runs (**Fig. 2**), thus allowing accurate peptide alignment and quantitative comparison of the samples. Statistical

analyses were carried out to identify differentially expressed peaks, resulting in the determination that 27% of the peaks showed differential expression (≥ 1.5 fold difference) between the two hemispheres (**Fig. 3**). As the variability between two biological synaptosomal preps was found to be about 10% (unpublished data), the observed differences were primarily attributable to the effects of cerebral ischemia and much less due to biological variability.

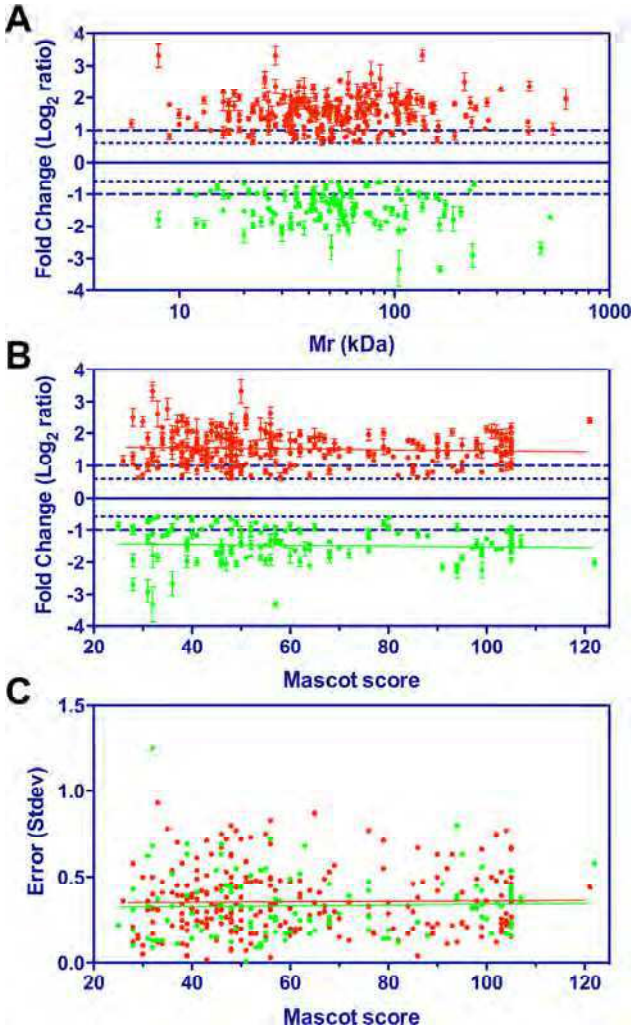

Fig. 5. Linear regression analysis of bias in label-free proteomics data. Expression data were plotted against protein mass and mascot score in panels A and B, respectively. Error values were plotted against mascot score in panel C. Linear regression analyses were performed on the up (red)- and down (green)-regulated proteins independently. Regression lines are plotted in panels B and C. Analyses of the regression slopes did not detect significant

departures from zero, indicating that there was no correlation between expression and protein size / mascot score or error and mascot score. A runs test indicated that there was no departure from linearity in the regression analysis of error versus mascot score. Furthermore, no significant differences were detected between the up and down regulated proteins in any of the analyses.

The differentially expressed peaks were then sequenced by re-injecting each fraction and analyzing with targeted nanoLC-MS/MS using an include list containing the masses and retention times of each targeted peak. The sequenced peptides were used to generate a list of ischemia-responsive proteins. A total of 371 proteins were identified as responsive to cerebral ischemia (hereafter referred to as either the IS dataset or IS proteins) (**Tables 1** and **2**). Two-thirds (68%) of these proteins were up-regulated and the remaining were down-regulated. Examples of up- and down-regulated proteins are shown in **Fig. 4**. A series of linear regression analyses were performed to ensure that the expression data was free of systematic bias. The results of the linear regression analyses indicate that the expression values were not correlated to protein mass (**Fig. 5A**) or Mascot score (**Fig. 5B**). Similarly, the measurement error was not correlated to Mascot score (**Fig. 5C**). These results indicate that the observed expression and error values are due to biological effects.

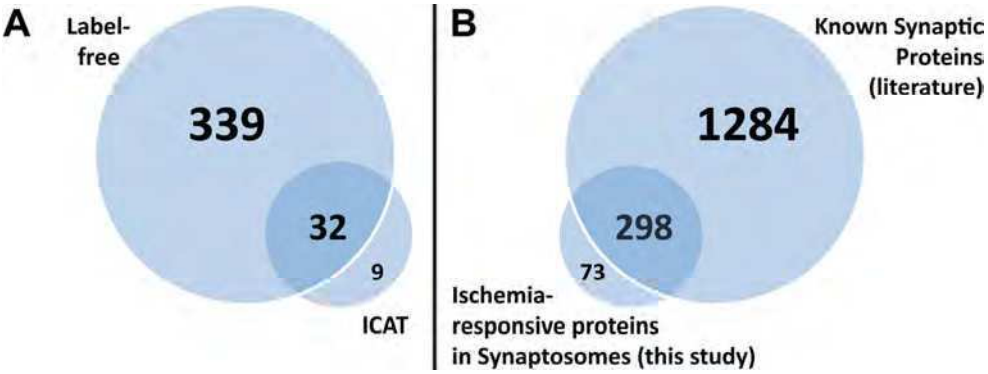

Fig. 6. (A) Venn diagram showing the number of differentially expressed proteins identified by label-free proteomics, ICAT proteomics (Costain et al. 2010) and both methods. (B) Venn diagram showing the overlap between the IS dataset using label-free proteomics (this study, 371 proteins) and the known synaptosomal proteins (1582 proteins) in the literature (Cheng et al. 2006, Morciano et al. 2005, Phillips et al. 2005, Schrimpf et al. 2005, Witzmann et al. 2005, Jordan et al. 2004, Peng et al. 2004, Stevens et al. 2003, Li et al. 2004).

To validate the purity of our synaptosomal preps, the IS proteins were searched against a known collection of synaptic protein datasets from recent literature that had been identified by proteomics. More than 80% of the IS proteins were found in these datasets (**Fig. 6B**), demonstrating that our preps are consistent with other synaptosomal datasets. However, the IS proteins corresponded to only about 23% of all the known synaptic proteins (**Fig. 6B**), which is also consistent with the fact that < 30% of the peaks were found as differentially expressed (**Fig. 3**). Literature mining through PubMed search identified that 56 proteins are known to be associated with middle cerebral artery occlusion model of ischemia (**Tables 1** and **2**).

Accession	Symbol	Exprs	Mito	synDB	MCAO
Q9CR67	Tmem33	3.3 ± 0.5		Yes	
Q06185	Atp5i	3.3 ± 0.7	Yes	Yes	
O54774	Ap3d1	3.3 ± 0.4		Yes	
P41216	Acsl1	2.8 ± 0.8	Yes	Yes	
XP_618960		2.7 ± 0.3	Yes	Yes	
Q5NCP0	Rnf43	2.6 ± 0.9	Yes	Yes	
O08709	Prdx6	2.6 ± 0.6	Yes	Yes	2
Q8BWF0	Aldh5a1	2.5 ± 0.2	Yes	Yes	
Q64487	Ptprd	2.5 ± 0.6		Yes	
Q68FF7	Slain1	2.5 ± 0.5		Yes	
Q8K2B3	Sdha	2.4 ± 0.4	Yes	Yes	
P16858	Gapdh	2.4 ± 0.6	Yes	Yes	5
P20108	Prdx3	2.4 ± 0.5	Yes	Yes	
P11531	Dmd	2.4 ± 0.5			
Q9QYB8	Add2	2.3 ± 0.4		Yes	
P15105	Glul	2.3 ± 0.5	Yes	Yes	8
Q9QYA2	Tomm40	2.3 ± 0.6	Yes	Yes	
Q8VE33	Gdap1l1	2.3 ± 0.3	Yes	Yes	
P11881	Itpr1	2.3 ± 0.4		Yes	
Q61207	Psap	2.3 ± 0.5	Yes	Yes	3
Q921L8	Galnt11	2.2 ± 0.4			
P10637	Mapt	2.2 ± 0.7		Yes	4
Q9CR61	Ndufb7	2.2 ± 0.1	Yes	Yes	
Q8BH59	Slc25a12	2.1 ± 0.8	Yes	Yes	
Q7TPR4	Actn1	2.1 ± 0.5	Yes	Yes	
P97493	Txn2	2.1 ± 0.4	Yes		9
Q9Z1G4	Atp6v0a1	2.1 ± 0.8		Yes	
P42228	Stat4	2.1 ± 0.1			
NP_001074599	Ogdhl	2.1 ± 0.5	Yes	Yes	
Q8BMS1	Hadha	2.1 ± 0.7	Yes	Yes	
Q9JLZ3	Auh	2 ± 0.4	Yes	Yes	
P81066	Irx2	2 ± 0.6			
Q3TRM8	Hk3	2 ± 0.4		Yes	
P09671	Sod2	2 ± 0.6	Yes	Yes	3
Q60931	Vdac3	2 ± 0.8	Yes	Yes	
Q8BMF4	Dlat	2 ± 0.6	Yes	Yes	
Q9Z2W1	Stk25	2 ± 0.5			1
P48318	Gad1	2 ± 0.6	Yes	Yes	5
P06745	Gpi	2 ± 0.2		Yes	1
O55143	Atp2a2	2 ± 0.7	Yes	Yes	
O08599	Stxbp1	2 ± 0.4	Yes	Yes	
Q9DCX2	Atp5h	2 ± 0.5	Yes	Yes	
P35486	Pdha1	2 ± 0.7	Yes	Yes	
P13595	Ncam1	2 ± 0.8		Yes	6
Q8R4N0	Clybl	2 ± 0.2	Yes		2

Accession	Symbol	Exprs	Mito	synDB	MCAO
P35803	Gpm6b	2 ± 0.8		Yes	
Q09666	Ahnak	2 ± 0.5			
Q61792	Lasp1	2 ± 0.8		Yes	
P20152	Vim	1.9 ± 0.4	Yes	Yes	9
Q99P72	Rtn4	1.9 ± 0.5		Yes	
P62874	Gnb1	1.9 ± 0.5	Yes	Yes	
Q08460	Kcnma1	1.9 ± 0.5		Yes	5
Q9CPP6	Ndufa5	1.9 ± 0.3	Yes	Yes	
Q8BIZ0	Pcdh20	1.9 ± 0.2			
Q9CR62	Slc25a11	1.9 ± 0.3	Yes	Yes	
Q8BVE3	Atp6v1h	1.9 ± 0.4	Yes	Yes	
P14094	Atp1b1	1.9 ± 0.9		Yes	
NP_444473	PRSS1	1.9 ± 0.7			
P18872	Gnao1	1.9 ± 0.8		Yes	
P60879	Snap25	1.9 ± 0.5		Yes	8
Q8VEA4	Chchd4	1.9 ± 0.5	Yes		
P57776-1	Eef1d	1.9 ± 0.4			
P14873	Map1b	1.8 ± 0.8		Yes	4
Q01279	Egfr	1.8 ± 0.6			5
Q9ERS2	Ndufa13	1.8 ± 0.5	Yes		
Q8VDD5	Myh9	1.8 ± 0.4		Yes	
Q80Z24	Negr1	1.8 ± 0.5		Yes	
Q925N0	Sfxn5	1.8 ± 0.3	Yes	Yes	
Q9UPR5	SLC8A2	1.8 ± 0.5	Yes	Yes	
Q8BFR5	Tufm	1.8 ± 0.4	Yes	Yes	
Q68FD5	Cltc	1.8 ± 0.7	Yes	Yes	
P17426	Ap2a1	1.8 ± 0.4		Yes	
P12960	Cntn1	1.8 ± 0.5		Yes	
Q9CR68	Uqcrfs1	1.8 ± 0.3	Yes	Yes	
Q91VD9	Ndufs1	1.8 ± 0.3	Yes	Yes	
Q62425	Ndufa4	1.8 ± 0.2	Yes	Yes	
Q8CAA7	Pgm2l1	1.8 ± 0.5		Yes	
P50516	Atp6v1a	1.8 ± 0.3	Yes	Yes	
Q9Z2I0	Letm1	1.8 ± 0.2	Yes	Yes	
Q96PV0	Syngap1	1.7 ± 0.5		Yes	
Q80TJ1	Cadps	1.7 ± 0.5		Yes	
P17742	Ppia	1.7 ± 0.3	Yes	Yes	1
P14231	Atp1b2	1.7 ± 0.6		Yes	
E9Q6J4	Ceacam3	1.7 ± 0.4			
Q9D6M3	Slc25a22	1.7 ± 0.4	Yes	Yes	
O55131	Sept7	1.7 ± 0.7		Yes	
P62761	Vsnl1	1.7 ± 0.6		Yes	
Q9D051	Pdhb	1.7 ± 0.3	Yes	Yes	
P14824	Anxa6	1.6 ± 0.3	Yes	Yes	
Q9QY06	Myo9b	1.7 ± 0.3			

Accession	Symbol	Exprs	Mito	synDB	MCAO
Q61644	Pacsin1	1.7 ± 0.3		Yes	
Q9D2G2	Dlst	1.7 ± 0.3	Yes	Yes	
Q9DBL1	Acadsb	1.7 ± 0.4	Yes	Yes	
P17182	Eno1	1.7 ± 0.5		Yes	
P63038	Hspd1	1.7 ± 0.7	Yes	Yes	10
Q9ULD0	OGDHL	1.7 ± 0.3	Yes	Yes	
Q8BKZ9	Pdhx	1.6 ± 0.3	Yes	Yes	
P62748	Hpcal1	1.6 ± 0.2		Yes	
P14211	Calr	1.6 ± 0.4		Yes	
P62482	Kcnab2	1.6 ± 0.5			
P40142	Tkt	1.6 ± 0.3		Yes	
P99029	Prdx5	1.6 ± 0.5	Yes	Yes	2
Q8VEM8	Slc25a3	1.6 ± 0.4	Yes	Yes	
P23818	Gria1	1.6 ± 0.4		Yes	5
O35526	Stx1a	1.6 ± 0.5		Yes	
P51830	Adcy9	1.6 ± 0.4		Yes	
XP_927453		1.6 ± 0.2			
P53994	Rab2a	1.6 ± 0.4	Yes	Yes	
P60710	Actb	1.6 ± 0.4	Yes	Yes	12
P31650	Slc6a11	1.6 ± 0.7		Yes	1
Q9Z2Q6	Sept5	1.6 ± 0.7	Yes	Yes	
Q99KI0	Aco2	1.6 ± 0.5	Yes	Yes	5
P46460	Nsf	1.6 ± 0.5		Yes	
Q6IFX4	Krt39	1.6 ± 0.5	Yes		
Q8R404	Qil1	1.6 ± 0.1	Yes	Yes	
O09111	Ndufb11	1.5 ± 0.7	Yes	Yes	
Q9DC69	Ndufa9	1.5 ± 0.3	Yes	Yes	
O88741	Gdap1	1.5 ± 0.5		Yes	
P07477	PRSS1	1.5 ± 0.4		Yes	
P17751	Tpi1	1.5 ± 0.3	Yes	Yes	
Q91V61	Sfxn3	1.5 ± 0.3	Yes	Yes	
P57780	Actn4	1.5 ± 0.5	Yes	Yes	
P97300	Nptn	1.5 ± 0.4		Yes	
Q99LC3	Ndufa10	1.5 ± 0.1	Yes	Yes	
P63017	Hspa8	1.5 ± 0.5	Yes	Yes	
Q99104	Myo5a	1.5 ± 0.5		Yes	1
Q9CQ69	Uqcrq	1.5 ± 0.4	Yes	Yes	
P46096	Syt1	1.5 ± 0.4		Yes	
Q8CAQ8	Immt	1.5 ± 0.3	Yes	Yes	
Q91WF3	Adcy4	1.5 ± 0.3			
Q64133	Maoa	1.5 ± 0.3	Yes	Yes	3
P97807	Fh	1.5 ± 0.2	Yes	Yes	1
Q9Z2I9	Sucla2	1.5 ± 0.2	Yes	Yes	
Q63810	Ppp3r1	1.5 ± 0.3			
O94925	GLS	1.5 ± 0.7	Yes	Yes	

Accession	Symbol	Exprs	Mito	synDB	MCAO
Q9R1T4	Sept6	1.5 ± 0.3		Yes	
P61922	Abat	1.5 ± 0.3	Yes	Yes	
Q61206	Pafah1b2	1.5 ± 0.4			
P06151	Ldha	1.5 ± 0.2	Yes	Yes	
P54227	Stmn1	1.5 ± 0.3		Yes	3
P31648	Slc6a1	1.4 ± 0.5		Yes	1
P28652	Camk2b	1.4 ± 0.3		Yes	
Q61548	Snap91	1.4 ± 0.2	Yes	Yes	
P48962	Slc25a4	1.4 ± 0.2	Yes	Yes	
P68254	Ywhaq	1.4 ± 0.2	Yes	Yes	
P50518	Atp6v1e1	1.4 ± 0.1	Yes	Yes	
Q8VHW2	Cacng8	1.4 ± 0.4		Yes	
O55125	Nipsnap1	1.4 ± 0.3	Yes	Yes	
O70566	Diaph2	1.4 ± 0.2	Yes	Yes	
P20936	RASA1	1.4 ± 0.2			
Q9ES97	Rtn3	1.4 ± 0.3		Yes	
P50114	S100b	1.4 ± 0.2		Yes	7
O08553	Dpysl2	1.4 ± 0.4	Yes	Yes	2
Q60930	Vdac2	1.4 ± 0.5	Yes	Yes	
Q02053	Uba1	1.4 ± 0.2		Yes	
Q9R0P9	Uchl1	1.4 ± 0.2		Yes	2
P10126	Eef1a1	1.4 ± 0.6	Yes	Yes	
Q60932	Vdac1	1.4 ± 0.3	Yes	Yes	
P06837	Gap43	1.4 ± 0.3		Yes	14
P62835	Rap1a	1.4 ± 0.2	Yes	Yes	
Q9D0F9	Pgm1	1.3 ± 0.2		Yes	
P62204	Calm1	1.3 ± 0.2		Yes	25
P47753	Capza1	1.3 ± 0.4		Yes	
P52480	Pkm2	1.3 ± 0.4	Yes	Yes	
Q9QZD8	Slc25a10	1.3 ± 0.4	Yes	Yes	
Q9EQF6	Dpysl5	1.3 ± 0.5	Yes		1
Q5SUA5	Myo1g	1.3 ± 0.2	Yes	Yes	
Q9D0S9	Hint2	1.3 ± 0.3	Yes	Yes	
Q62261	Sptbn1	1.3 ± 0.2		Yes	
Q8BVI4	Qdpr	1.3 ± 0.2	Yes	Yes	
O70443	Gnaz	1.3 ± 0.2	Yes	Yes	
P18760	Cfl1	1.3 ± 0.3	Yes	Yes	
Q62315	Jarid2	1.3 ± 0.2			
Q03963	Eif2ak2	1.3 ± 0.2			
P35802	Gpm6a	1.3 ± 0.4		Yes	
Q9D6R2	Idh3a	1.3 ± 0.2	Yes	Yes	1
O08749	Dld	1.3 ± 0.4	Yes	Yes	
P38647	Hspa9	1.3 ± 0.4	Yes	Yes	1
O88737	Bsn	1.3 ± 0.3		Yes	
P70268	Pkn1	1.3 ± 0.3			

Accession	Symbol	Exprs	Mito	synDB	MCAO
Q61879	Myh10	1.3 ± 0.3		Yes	
P62814	Atp6v1b2	1.3 ± 0.2		Yes	
P07901	Hsp90aa1	1.3 ± 0.3	Yes	Yes	
P63328	Ppp3ca	1.3 ± 0.3	Yes	Yes	
P56382	Atp5e	1.2 ± 0.2	Yes	Yes	
P99028	Uqcrh	1.2 ± 0	Yes	Yes	
P05201	Got1	1.2 ± 0.2	Yes	Yes	
P16277	Blk	1.2 ± 0.3		Yes	
Q9CQA3	Sdhb	1.2 ± 0.3	Yes	Yes	
P07146	Prss2	1.2 ± 0.2			
Q9WV55	Vapa	1.2 ± 0.3		Yes	
P28663	Napb	1.2 ± 0.2		Yes	
O35658	C1qbp	1.1 ± 0.2	Yes	Yes	
Q9CZW5	Tomm70a	1.1 ± 0.2	Yes	Yes	
Q9Z0J4	Nos1	1.1 ± 0.3	Yes	Yes	66
Q80XN0	Bdh1	1.1 ± 0.2	Yes	Yes	
P34884	Mif	1.1 ± 0.2		Yes	3
Q8K314	Atp2b1	1.1 ± 0.3		Yes	
Q640R3	Hepacam	1.1 ± 0.1		Yes	
Q5SWU9	Acaca	1.1 ± 0.1	Yes	Yes	
Q00690	Sele	1.1 ± 0			26
A2AJ76	Hmcn2	1 ± 0.3			
Q9JI46	Nudt3	1 ± 0.2		Yes	
Q6PCP5	Mff	1 ± 0.1	Yes	Yes	
O70283	Wnt2b	1 ± 0.2			
P70295	Aup1	1 ± 0.2			
Q80Y86	Mapk15	1 ± 0.2		Yes	
Q9CQ54	Ndufc2	1 ± 0.2	Yes	Yes	
P00405	Mtco2	1 ± 0.3	Yes	Yes	
P63082	Atp6v0c	1 ± 0.2			
Q9D8W7	Ociad2	1 ± 0.2	Yes		
XP_922613	Spnb5	1 ± 0.3			
P43006	Slc1a2	1 ± 0.2		Yes	10
Q9R111	Gda	1 ± 0.2		Yes	
Q9CQI3	Gmfb	0.9 ± 0.3		Yes	
XP_922643		0.9 ± 0.1			
O35857	Timm44	0.9 ± 0.2	Yes		
Q8BM92	Cdh7	0.9 ± 0.1		Yes	
P56564	Slc1a3	0.8 ± 0.2	Yes	Yes	
O54983	Crym	0.9 ± 0.1	Yes		
NP_082646	Pot1b	0.9 ± 0.2			
Q9JKR6	Hyou1	0.9 ± 0.2			
Q9CQH3	Ndufb5	0.9 ± 0.2	Yes		
P48320	Gad2	0.9 ± 0.1		Yes	1
Q61735	Cd47	0.9 ± 0.1			1

Accession	Symbol	Exprs	Mito	synDB	MCAO
Q9H4G0	EPB41L1	0.9 ± 0.2		Yes	
P08228	Sod1	0.9 ± 0.2	Yes	Yes	10
P62137	Ppp1ca	0.9 ± 0.3		Yes	
Q62277	Syp	0.9 ± 0.2		Yes	30
Q9QZ83	Actg1	0.9 ± 0.2	Yes	Yes	
A8E4K7	Pcdhb8	0.8 ± 0.1			
Q8K183	Pdxk	0.8 ± 0.2			2
P08556	Nras	0.8 ± 0.2	Yes	Yes	
Q61194	Pik3c2a	0.8 ± 0.3			
Q9DCS9	Ndufb10	0.8 ± 0.1	Yes	Yes	
Q62420	Sh3gl2	0.8 ± 0.2		Yes	
P48771	Cox7a2	0.8 ± 0.3	Yes		
O35728	Cyp4a14	0.8 ± 0.1			
Q6GQS1	Slc25a23	0.8 ± 0.3	Yes		
Q9CWZ7	Napg	0.7 ± 0.1	Yes	Yes	
Q99JY0	Hadhb	0.7 ± 0.1	Yes	Yes	
Q8K0T0	Rtn1	0.7 ± 0.2		Yes	
P0CG49	Ubb	0.7 ± 0	Yes	Yes	17
P84091	Ap2m1	0.7 ± 0.1	Yes	Yes	
P70335	Rock1	0.7 ± 0.2			
O09112	Dusp8	0.7 ± 0.1			
Q3UK37		0.7 ± 0.1			
Q8BLF1	Nceh1	0.7 ± 0.2			
Q76MZ3	Ppp2r1a	0.6 ± 0	Yes	Yes	
Q8BGZ1	Hpcal4	0.6 ± 0.2		Yes	
B9EJA4	Clasp2	0.6 ± 0.1			
P05202	Got2	0.3 ± 1.6	Yes	Yes	1

Table 1. List of up-regulated proteins in the IS dataset. The expression (Exprs) of each proteins is provided (mean ± SD, n = 3), as well as their presence in the mitochondria (Mito) or synapse (SynDB). The number of citations in PubMed that have associated each proteins with stoke (MCAO) are also provided.

To further characterize the IS dataset, the proteins were categorized into biological processes and subcellular localizations using a combination of Panther, Uniprot and other datasets (Taylor et al. 2003). Categorization by biological processes showed that the majority of the IS proteins are involved in transport, signal transduction, intracellular trafficking and carbohydrate metabolism (**Fig. 7A**). Additionally, up-regulated proteins were involved in the processes of immunity/defense, cell adhesion and neurogenesis. Subcellular classification mainly categorized the proteins into mitochondrial, cell membrane, cytoplasmic and membrane/cytoplasmic localizations (**Fig. 7B**). Consistent with our previous report (Costain et al. 2010), approximately half (51%) of the IS dataset were mitochondrial proteins (**Fig. 7B**), whereas < 25% of known synaptosomal proteins are mitochondrial. These changes were mainly due to mitochondrial oxidoreductases involved in electron transport and proteins involved in the TCA cycle, suggesting severe deficits in the capacity of the mitochondria to produce energy. About 20% of the identified ischemic

Accession	Symbol	Exprs	Mito	SynDB	MCAO
Q920I9	Wdr7	-3.3 ± 0.2		Yes	
Q8R1B4	Eif3c	-3.3 ± 1.3		Yes	
P42356	PI4KA	-2.9 ± 0.6		Yes	
Q8R071	Itpka	-2.7 ± 0.5		Yes	
P67778	Phb	-2.3 ± 0.4	Yes		
P19783	Cox4i1	-2.3 ± 0.8		Yes	
Q4U256	Ank3	-2.2 ± 0.6		Yes	
Q9DBG3	Ap2b1	-2.2 ± 0.5	Yes	Yes	
P51881	Slc25a5	-2.1 ± 0.5	Yes		
Q3V1U8	Elmod1	-2.1 ± 0.5	Yes	Yes	
P58281	Opa1	-2.1 ± 0.3		Yes	
Q64516	Gyk	-2.1 ± 0.4		Yes	
Q99LY9	Ndufs5	-2 ± 0.6			
P54285	Cacnb3	-2 ± 0.7	Yes	Yes	
Q8VD37	Sgip1	-2 ± 0.5		Yes	
P49615	Cdk5	-2 ± 0.4	Yes	Yes	
Q62159	Rhoc	-2 ± 0.6	Yes	Yes	2
Q9DB77	Uqcrc2	-2 ± 0.6		Yes	
Q9DCT2	Ndufs3	-2 ± 0.3	Yes	Yes	
P21803	Fgfr2	-1.9 ± 0		Yes	
Q7TQD2	Tppp	-1.9 ± 0.5	Yes	Yes	
Q64521	Gpd2	-1.9 ± 0.6	Yes	Yes	
P08249	Mdh2	-1.9 ± 0.2		Yes	
Q91WS0	Cisd1	-1.9 ± 0.7		Yes	
Q5DU25	Iqsec2	-1.9 ± 0.4			
Q03265	Atp5a1	-1.9 ± 0.2	Yes	Yes	
Q9CPQ1	Cox6c	-1.8 ± 0.5	Yes		
Q04447	Ckb	-1.8 ± 0.3	Yes	Yes	
P61161	Actr2	-1.8 ± 0.2	Yes	Yes	
Q9D6J6	Ndufv2	-1.8 ± 0.5	Yes		
Q5NVN0	PKM2	-1.8 ± 0.4			
Q6PIC6	Atp1a3	-1.7 ± 0.4			
Q8QZT1	Acat1	-1.7 ± 0.6			
O08539	Bin1	-1.7 ± 0.7			
Q9JHU4	Dync1h1	-1.7 ± 0.3	Yes	Yes	
Q91VR2	Atp5c1	-1.7 ± 0.4	Yes	Yes	
P14618	PKM2	-1.7 ± 0.5		Yes	
O88935	Syn1	-1.6 ± 0.4			
Q9D0K2	Oxct1	-1.6 ± 0.5	Yes	Yes	
Q61330	Cntn2	-1.6 ± 0.7	Yes	Yes	
Q91XV3	Basp1	-1.6 ± 0.5		Yes	
Q3V1L4	Nt5c2	-1.6 ± 0.3	Yes	Yes	
Q8BG39	Sv2b	-1.6 ± 0.4			
P61982	Ywhag	-1.6 ± 0.3	Yes	Yes	
Q80ZF8	Bai3	-1.6 ± 0.4		Yes	

Accession	Symbol	Exprs	Mito	SynDB	MCAO
P17427	Ap2a2	-1.6 ± 0.3	Yes	Yes	
Q9DBF1	Aldh7a1	-1.6 ± 0.4	Yes	Yes	8
P39053	Dnm1	-1.5 ± 0.2	Yes	Yes	
P70404	Idh3g	-1.5 ± 0.1	Yes	Yes	
P99024	Tubb5	-1.5 ± 0.3	Yes	Yes	
P12787	Cox5a	-1.5 ± 0.3	Yes	Yes	
Q8CI94	Pygb	-1.5 ± 0.6		Yes	
XP_001006010		-1.5 ± 0.1	Yes	Yes	
Q9QXV0	Pcsk1n	-1.5 ± 0.3		Yes	
P68368	Tuba4a	-1.5 ± 0.3		Yes	
Q2EMV9	Parp14	-1.5 ± 0.3	Yes	Yes	1
P05064	Aldoa	-1.5 ± 0.3		Yes	
NP_031573	Sirpa	-1.4 ± 0.4		Yes	
O88342	Wdr1	-1.4 ± 0.4	Yes	Yes	
Q9D0M3	Cyc1	-1.4 ± 0.2		Yes	
Q9QWI6	Srcin1	-1.4 ± 0.5			
Q69ZK9	Nlgn2	-1.4 ± 0.2		Yes	
P56480	Atp5b	-1.4 ± 0.2		Yes	
Q8CIV2	ORF61	-1.4 ± 0.3	Yes	Yes	
Q3UM45	Ppp1r7	-1.4 ± 0.5	Yes	Yes	
O55100	Syngr1	-1.4 ± 0.2	Yes	Yes	
P97797	Sirpa	-1.3 ± 0.3	Yes	Yes	
P51174	Acadl	-1.3 ± 0.3			
Q9CZ13	Uqcrc1	-1.3 ± 0.4			
BAE40217	Tubb5	-1.3 ± 0.3		Yes	5
AAA40509	Tubb4	-1.3 ± 0.4		Yes	
Q9WUM5	Suclg1	-1.3 ± 0.3			
Q8CHC4	Synj1	-1.3 ± 0.4	Yes	Yes	
P14152	Mdh1	-1.3 ± 0.2	Yes	Yes	
P17710	Hk1	-1.2 ± 0.2			
P23116	Eif3a	-1.2 ± 0.1		Yes	
O43837	IDH3B	-1.2 ± 0.4	Yes	Yes	
Q9CZU6	Cs	-1.2 ± 0.3		Yes	
XP_889898		-1.1 ± 0.3	Yes	Yes	
Q6NXI6	Rprd2	-1.1 ± 0.2	Yes	Yes	
NP_001013813	Gm5468	-1.1 ± 0.1	Yes	Yes	
P11627	L1cam	-1.1 ± 0.3	Yes	Yes	
O77784	IDH3B	-1.1 ± 0.4	Yes	Yes	
Q9CPU4	Mgst3	-1.1 ± 0.1	Yes	Yes	
Q8R570	Snap47	-1.1 ± 0.3		Yes	
Q8TCB6	OR51E1	-1.1 ± 0.2		Yes	
NP_082221	Csl	-1.1 ± 0.4	Yes	Yes	
Q9WUM4	Coro1c	-1.1 ± 0.1	Yes	Yes	
P10649	Gstm1	-1.1 ± 0.2		Yes	
Q9DB20	Atp5o	-1 ± 0.2	Yes		

Accession	Symbol	Exprs	Mito	SynDB	MCAO
Q9R0N5	Syt5	-1 ± 0.3	Yes	Yes	
Q9QXY2	Srcin1	-1 ± 0.2		Yes	
Q9CQY6	LOC675054	-1 ± 0.2	Yes	Yes	
Q3TC72	Fahd2	-1 ± 0.4	Yes	Yes	
Q8BK30	Ndufv3	-1 ± 0.2		Yes	1
Q9EQ20	Aldh6a1	-1 ± 0.3		Yes	
P30275	Ckmt1	-1 ± 0.2	Yes	Yes	1
Q8CHU3	Epn2	-1 ± 0.3	Yes	Yes	
O35643	Ap1b1	-0.9 ± 0.2	Yes	Yes	
O35874	Slc1a4	-0.9 ± 0.2		Yes	
P56391	Cox6b1	-0.9 ± 0.1	Yes	Yes	
A2AGT5	Ckap5	-0.9 ± 0.2	Yes	Yes	
P19536	Cox5b	-0.9 ± 0.1		Yes	
Q60597	Ogdh	-0.9 ± 0.3		Yes	
Q3TMW1	Ccdc102a	-0.9 ± 0.2		Yes	4
NP_570954	IDH3B	-0.9 ± 0.4		Yes	
P61205	Arf3	-0.9 ± 0.2	Yes	Yes	
Q9DC70	Ndufs7	-0.9 ± 0.3	Yes	Yes	
Q61124	Cln3	-0.8 ± 0.2	Yes	Yes	
Q99LC5	Etfa	-0.8 ± 0.1			
P63040	Cplx1	-0.8 ± 0.1	Yes	Yes	
Q8BH44	Coro2b	-0.7 ± 0.1	Yes	Yes	6
Q9CXZ1	Ndufs4	-0.7 ± 0.1		Yes	
P49025	Cit	-0.7 ± 0.1	Yes	Yes	
Q7TQF7	Amph	-0.7 ± 0.2	Yes	Yes	
P48678	Lmna	-0.7 ± 0.1	Yes	Yes	
O89053	Coro1a	-0.6 ± 0.1		Yes	
Q8BUV3	Gphn	-0.6 ± 0.1		Yes	
P35831	Ptpn12	-0.6 ± 0.1			

Table 2. List of down-regulated proteins in the IS dataset. The expression (Exprs) of each proteins is provided (mean ± SD, n = 3), as well as their presence in the mitochondria (Mito) or synapse (SynDB). The number of citations in PubMed that have associated each proteins with stoke (MCAO) are also provided.

proteins were classified as membrane/cytoplasmic, i.e., they exist in both cell membranes and cytoplasm. These 73 proteins consist of membrane trafficking proteins, transfer/carrier proteins, calcium-binding proteins, cytoskeletal proteins and transporters and are known to be involved in the processes of vesicle trafficking and synaptic transmission. Of the remaining identified ischemic proteins, 11% were classified as membrane-only and 9% as cytoplasm-only (**Fig. 7B**). The membrane-only proteins consist of transporters, adhesion molecules and cytokine receptors, which are known to be involved in the processes of cell adhesion, cell communication, signal transduction, neurogenesis and transport. The cytoplasm-only proteins consist of cytoskeletal proteins, enzymes (e.g., hydrolases, kinases, phosphatases) and G-proteins and are involved in the processes of signal transduction, cell structure maintenance and cell motility.

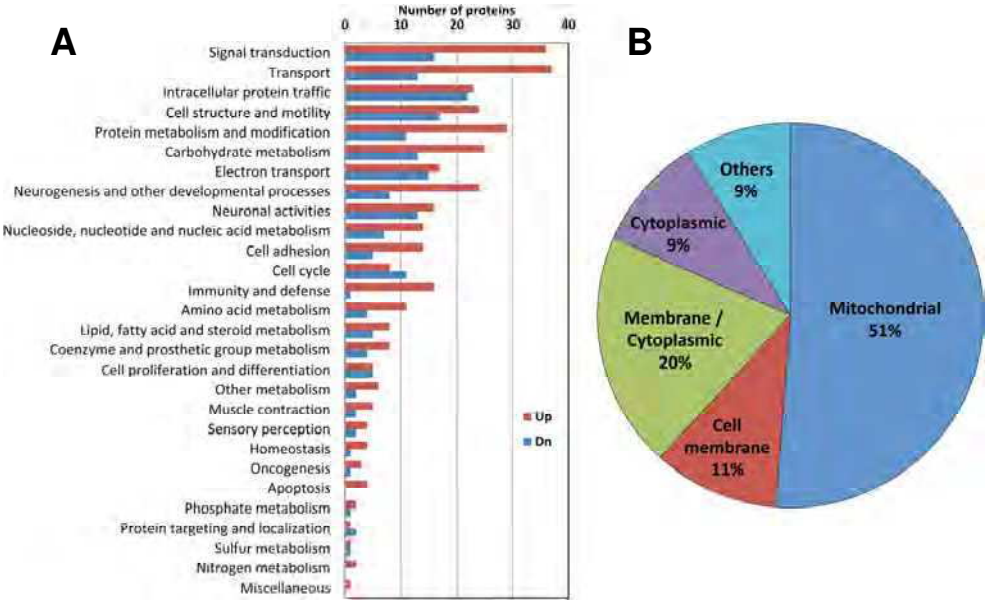

Fig. 7. Classification of differentially expressed proteins after targeted identification using nanoLC-MS/MS. (A) Protein classification by biological processes using the Panther classification system. (B) Protein classification by subcellular localizations using Panther, Uniprot and a dataset from Taylor et al. (2003).

3.2 Statistical analysis of Gene Ontology meta data

Graphical and statistical analyses of the Gene Ontology (GO) annotations were performed using the BiNGO 2.4.4 plugin for Cytoscape 2.8.2. This analysis involves gathering the GO meta data associated with the IS proteins, and determining if any annotations are statistically over-represented for each annotation category. BiNGO makes use of the hierarchical structure of the GO database to produce a graphical representation of the significantly over-represented ontologies, enabling the depiction of the parent-child relationships of the annotations. **Fig. 8** is the graphical representation of the relative positions of the terms in the GO hierarchy, with the degree of significance indicated according to color (white nodes are not significant). The size of each node (area) is proportional to the number of proteins annotated to each node. The major, significant *cellular component* ontologies (**Fig. 8A**) are cytoplasm, mitochondrion, cytoskeleton, plasma membrane, cytoplasmic membrane-bounded vesicle, Golgi apparatus, endoplasmic reticulum and vacuole. This list indicates that cerebral ischemia induces dramatic alterations in the proteomes of organelles that are involved in regulating cell death/survival processes. This is further supported by the *molecular function* ontologies (**Fig. 8C**) that are significantly enriched in terms such as kinase activity, transporter activity, antioxidant activity, electron carrier activity and nucleotide binding. Additionally, the enriched *biological process* ontologies (**Fig. 8B**) are dominated by a variety of metabolic processes, as well as transport, cellular component organization,

cellular homeostasis, response to stress and response to external stimulus. Taken together, the gene ontology information paints a picture of a dynamic proteome that is responding to highly stressful injury.

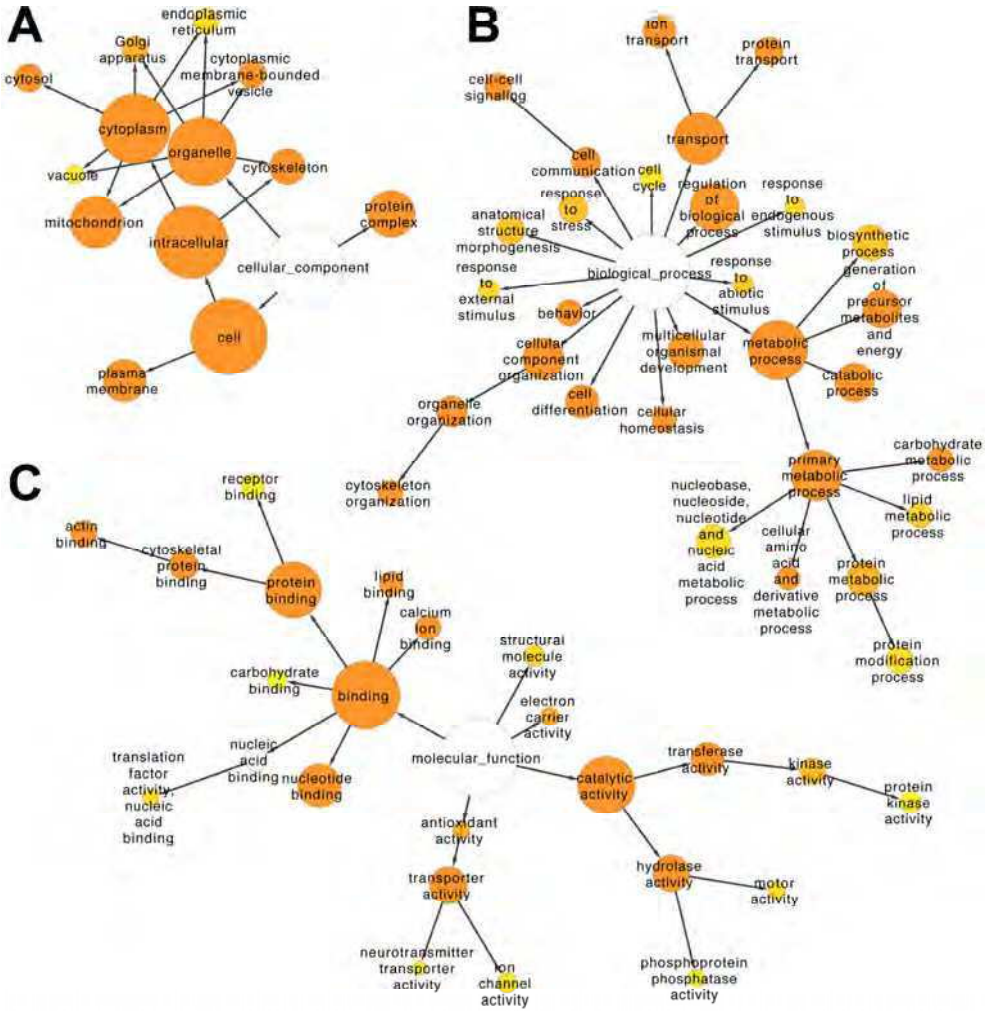

Fig. 8. Statistical analysis of Gene Ontology meta data. Statistical analysis of the Gene Ontology classification of the IS dataset was performed using the BiNGO plugin in Cytoscape. Graphical representations of significantly enriched ontologies are presented for cellular component (A), biological process (B) and molecular function (C).

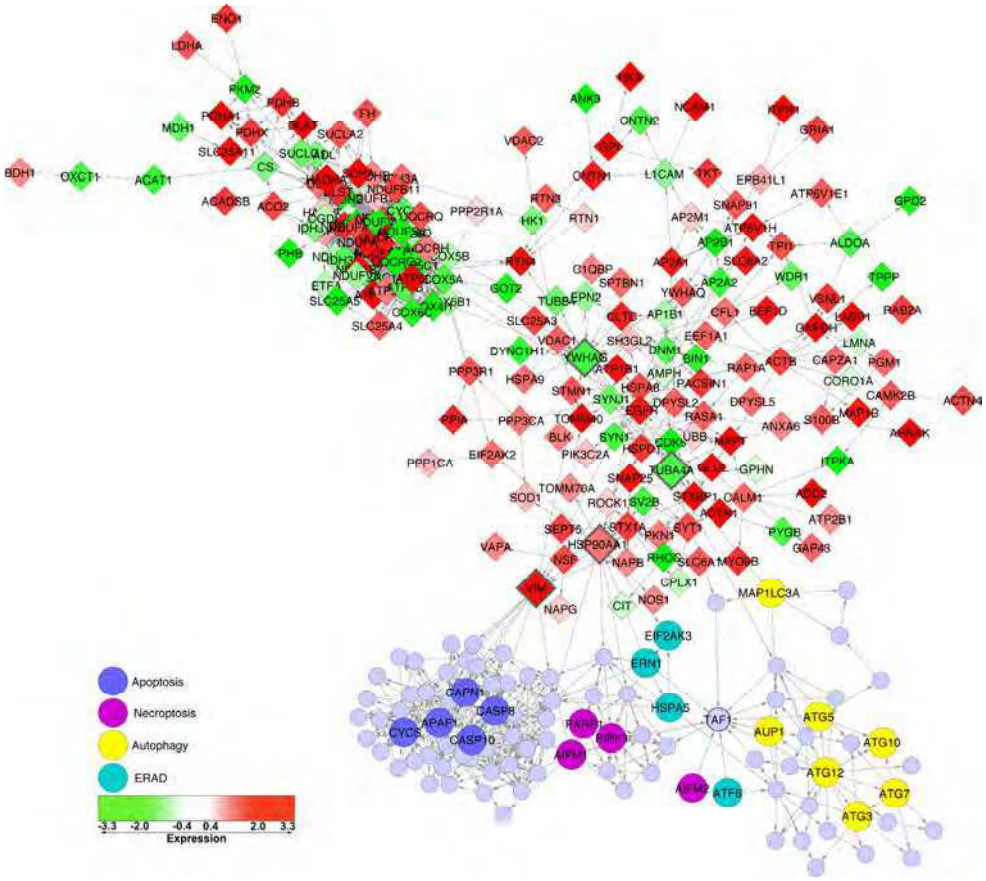

Fig. 9. Identification of therapeutic targets using a network of interactions between the IS dataset and key proteins involved in cell death mechanisms. Networks were constructed with MiMI from regulators of cell death pathways for apoptosis (Map3k14, Endog, Aifm1, Apaf1, Cycs, Capn1, Casp8, Casp10), autophagy (Aup1, Map1lc3a, Atg3, Atg5, Atg7, Atg10, Atg12), necroptosis (Aifm1, Aifm2, Parp1, Ripk1) and ER stress (ERAD; Ern1, Ern2, Hspa5, Atf6, Eif2ak3). These networks were joined with an ischemia network constructed of interacting proteins in the IS dataset (diamonds). The expression of the ischemic synaptic proteins is mapped onto the nodes according to the scale provided, with red and green representing up- and down-regulation, respectively. Key proteins (highlighted with bold node borders) for joining the cell death networks to the ischemia network (Hsp90aa1, Tuba4a, Vim) as well as highly integrated proteins (Ywhag and Taf1) were identified.

3.3 Comparison with ischemic-responsive proteins identified by ICAT

We recently identified 41 ischemia-responsive synaptosomal proteins at 20 h using ICAT-based nanoLC-MS/MS proteomics. While the ICAT-based method exhibited a high quantitative reproducibility, quantitative accuracy, and a wide dynamic range (Costain et al. 2010), it did not provide a very comprehensive analysis of the proteins. A comparison between the label-free and ICAT methods is shown in **Table 3**. While both methods have high quantitative reproducibility, the label-free method identified about 5-times more proteins and peptides in a synaptosome prep than the ICAT method. In addition, the number of peptides per protein and proteome coverage was significantly higher using the label-free method. The label-free method also showed higher peptide scores and identified several cysteine-free proteins. The label-free method identified 32 of the proteins that were also identified by ICAT (**Fig. 6A**) and the majority (80%) of their expressions values (i.e., fold change in response to MCAO) were in agreement between the two methods. Thus, while both methods are quantitatively comparable, the label-free approach provided a much more comprehensive coverage of the proteome and addressed some of the limitations of ICAT, including the detection of cysteine-free proteins.

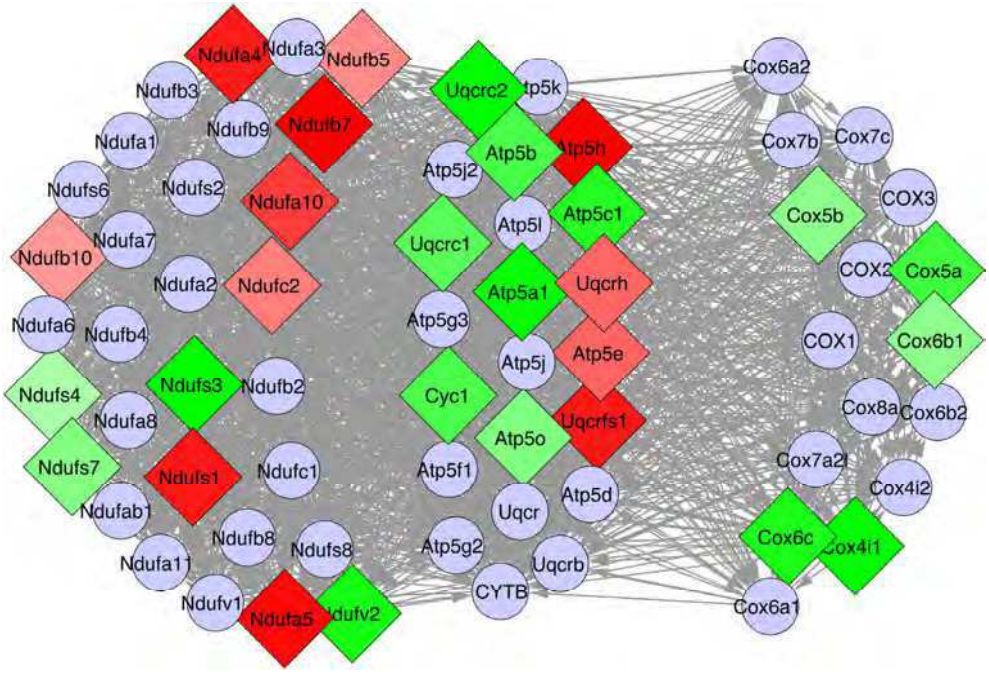

Fig. 10. Cerebral ischemia disrupts synaptosomal oxidative phosphorylation. An interaction network was constructed from proteins involved in oxidative phosphorylation using MiMI. The network segregated into proteins from 3 groups: complex I (NADH dehydrogenase (ubiquinone), complex IV (cytochrome-C oxidase) and complex V (ATP synthesis).

	Label-free	ICAT	*t-test*
Mean number of ions detected by nanoLC-MS per sample	>12,000	<4,000	*p<0.0001*
Quantitative reproducibility (mean coefficient of variance)	10%	9%	*ns*
Total unique proteins identified	371	41	
Peptides per protein	3.9	1.2	*p<0.0001*
Protein coverage (%)	15%	4.4%	*p<0.0001*
Peptide scores	71	32	*p<0.0001*
Number of cysteine-free proteins	13	N/A	

Table 3. Statistical comparison of label-free and ICAT based nanoLC-MS proteomics.

3.4 Protein interaction analysis

In an effort to identify proteins that are important in mediating ischemia-induced cell death, interaction networks were constructed using the MiMI plugin in Cytoscape. Key proteins involved in initiating the four major active cell death mechanisms were identified and stringent interaction networks were individually constructed. Additionally, a network of interactions among the proteins in the IS dataset was constructed, which resulted in the generation of a network consisting of 203 proteins (IS network). The cell death networks were merged with the IS network, resulting in the identification of a number of proteins that are likely to be important mediators of synaptic pathology and cell death (**Fig. 9**). This analysis revealed a strong degree of association between apoptosis and necroptosis, but little direct interaction with autophagy. In comparison, ER associated degradation (ERAD) was associated with both necroptosis and autophagy. **Fig. 9** indicates that the IS network is connected to apoptosis primarily through the vimentin (Vim) protein, whereas the necroptosis and ERAD networks are connected to the IS network in large part due to Hsp90aa1. In comparison, the autophagy network was connected to the IS network through Tuba4a. Additionally, the 14-3-3 protein Ywhag was revealed to be a highly connected protein within the IS network and the transcription factor Taf1 is a point of convergence for the ERAD, autophagy and necroptosis pathways.

As mentioned, many of the IS proteins are involved in a group of activities that are of obvious importance to cellular metabolism and signaling. These functionalities are highly important in maintaining cellular homeostasis as well as in deciding cellular fate during injurious conditions. **Fig. 10** is a graphical representation of the interactions among the proteins involved in the process of oxidative phosphorylation. The proteins segregated into three groups with related functions: cytochrome-C oxidase activity, NADH dehydrogenase (ubiquinone) activity and hydrogen ion transmembrane transporter activity. The expression of the proteins reveals that the Cox proteins were universally down-regulated, whereas proteins in the other groups exhibited more varied effects. **Fig. 11A** is a network of the proteins involved in glycolysis – gluconeogenesis. The figure demonstrates that there is widespread up-regulation of glycolytic proteins, with down-regulation of only two proteins. Similarly, **Fig. 11B** indicates that there is widespread up-regulation of proteins with anti-oxidant activity. Interestingly, two of the proteins identified in **Fig. 9**, Hsp90aa1 and Taf1, are also involved in the antioxidant response. The results depicted in **Fig. 11** clearly demonstrate that the ischemic synaptosomal proteome is actively engaged in an attempt to counteract the effects of cerebral ischemia, namely energy depletion and oxidative damage.

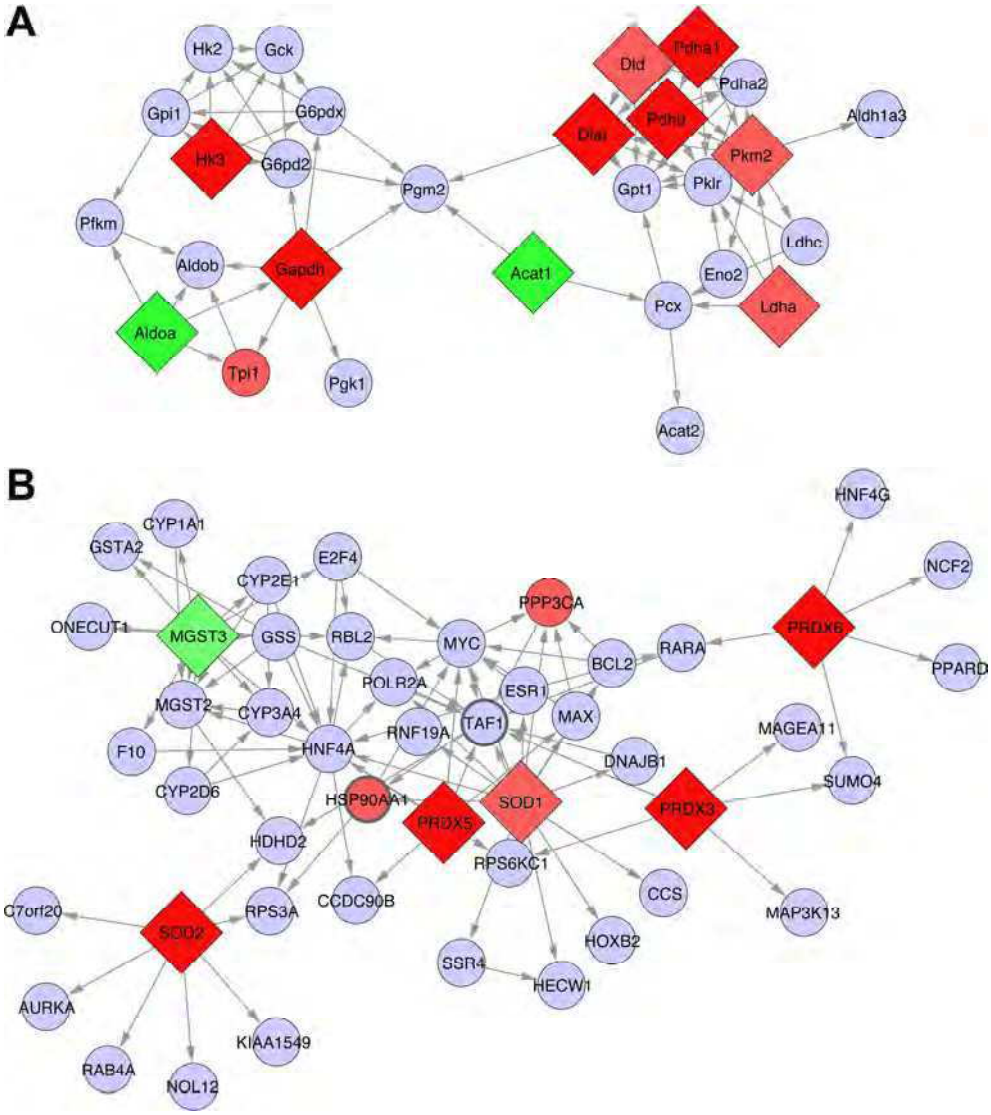

Fig. 11. Interaction network analysis demonstrates cellular responses to energy depletion and oxidative stress. Panel A is a network of proteins involved in glycolysis - gluconeogenesis, showing the up-regulation of proteins involved in this process. Panel B is a network showing the up-regulation of proteins with anti-oxidative properties.

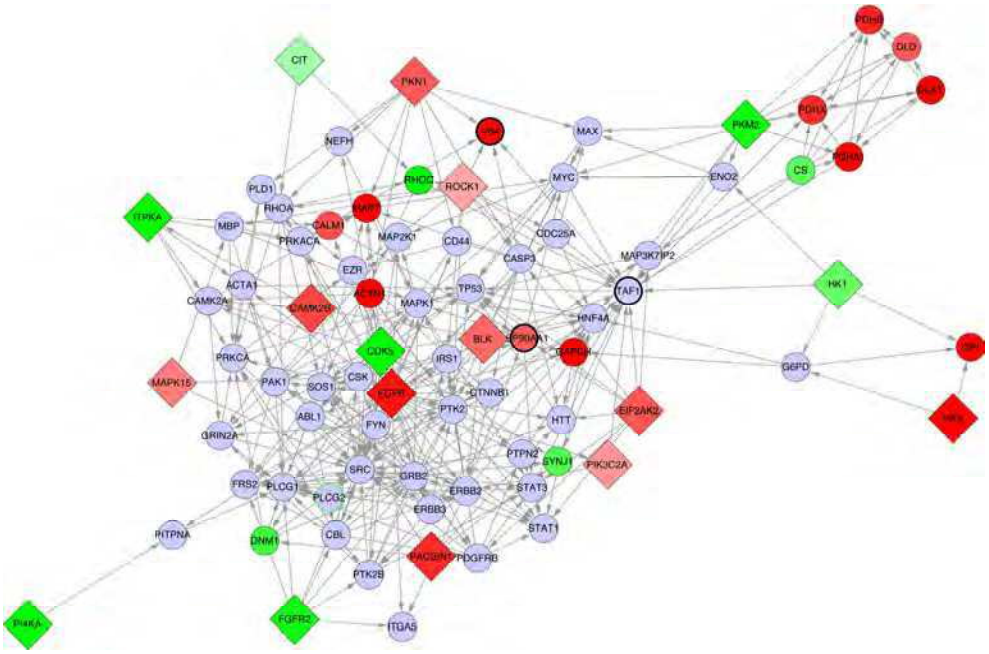

Fig. 12. Interaction network of ischemia regulated protein kinases. The network shows the regulated kinases (diamonds) interact with a subset of 16 other proteins in the IS dataset.

Actively regulated cell death processes rely on a variety of cellular signaling cascades, typically involving specific protein kinases. We found that the expression of 24 protein kinases were altered in post-ischemic synaptosomes and constructed an interaction network from this subset of proteins (**Fig. 12**). The resultant kinase network included 17 of the 24 kinases as well as 16 non-kinase synaptosomal proteins that were in the IS dataset. Interestingly, three of the key proteins identified in **Fig. 9** were present in the kinase network (Hsp90aa1, Vim and Taf1), supporting a broad role for these proteins in ischemic pathology. Interestingly, a group of proteins constituting the pyruvate dehydroxylase complex (Pdhb, Pdha1, Pdhx, Dld and Dlat), which links glycolysis and the tricarboxylic acid (TCA) cycle, were up-regulated, while citrate synthase (Cs) was down-regulated. The figure confirms that a wide variety of signaling pathways are affected by cerebral ischemia.

4. Discussion

The aim of this study is to characterize the effects of cerebral ischemia on the synaptic proteome and to examine the functional consequences of these alterations with particular emphasis on their relevance to neuronal cell death processes. As outlined, cellular protein levels are determined by the balance between synthesis and degradation, which is affected by a multitude of factors including: transcription, translation, proteases activity, and post-translational modifications. Ischemic conditions complicate the matter by causing dysfunction in the proteosome (DeGracia et al. 2002) and endoplasmic reticulum (Ge et al. 2007). Thus, gene expression data alone is a poor indicator of post-ischemic cellular protein levels. Furthermore focusing on the synapse adds the prospect of intracellular transport

mechanisms and localized translation further blurring the association between transcription and synaptic protein levels (Zhao et al. 2005, Vanderklish & Bahr 2000, Havik et al. 2003). As a result of these factors, the best approach for determining post-ischemic synaptic protein levels is to perform a direct assessment using proteomic methodologies.

4.1 Cerebral ischemia-induced alterations in the synaptic proteome

Here, we determined the proteomic response of the mouse brain synapse to cerebral ischemia by performing an analysis of mouse brain synaptosomes. Using a label-free nanoLC-MS/MS method, we identified 371 synaptosomal proteins that were altered 20 hrs after cerebral ischemia (**Table 3**), representing ≈ 27% of the total peaks detected. Linear regression analysis was used to exclude the possible influence of systemic bias on expression due to protein size and MASCOT score (**Fig. 5**). The purity of the synaptosomal prep was validated by the determination that > 80% of the IS dataset were previously characterized as being localized in the synapse (**Fig. 6**). Consistent with our previous study, the majority of the IS proteins were localized in the mitochondria (Costain et al. 2010), and the localization of the remaining proteins was consistent with the synaptic compartment. Furthermore, literature mining of PubMed indicated that only ≈ 15% of the IS proteins were associated with the MCAO model of cerebral ischemia. A statistical analysis of the ontological classification of the IS dataset revealed a number of important details (**Fig. 8**). Firstly, the significant enrichment of proteins located in the mitochondria, endoplasmic reticulum and Golgi apparatus indicate the importance of these structures in mediating post-ischemic neuronal function. Secondly, significantly enriched molecular function ontologies include kinase, transport, antioxidant and electron carrier activity. These functions are related to metabolism, and are consistent with tissues responding to catastrophic energy depletion. Lastly, the significantly enriched biological process ontologies were also associated with metabolism and stress responses. The present results, obtained using label-free nanoLC-MS/MS, are largely in agreement with our previous ICAT-based proteomics study (**Table 3**). The consistency between these datasets reflects the reproducibility and purity of synaptosomal preparations, as well as the proteomic methodologies. Furthermore, the label-free method produced a more comprehensive dataset than the ICAT method, exhibiting greater protein coverage, peptide scores and the ability to identify cysteine-free proteins.

4.2 Interaction network analysis

In an effort to place the observed alterations in the IS dataset into biological context, a variety of protein interaction analyses were performed. Interaction networks can be constructed from a variety of data types, such as protein-protein, protein-DNA and genetic interactions. The value of examining such interactions is that the overall biochemical function of proteins or DNA is a product of the interactions in which they participate. Thus, analyzing functional interactions enables the construction of signaling pathways or interaction networks that are capable of modeling a system or interpreting systematic responses to a given perturbation. In the present study, we used our observed systematic alterations in synaptosomal protein expression, and protein-protein interaction analyses to aid in interpreting the net effect of ischemia on the biological system (synapses and neurons). Furthermore, we integrated our observations in IS synaptosomes with key proteins in cell death pathways that are highly predictive of cell fate. Lastly, we focused on certain subsets of proteins to produce interaction networks that provided insight into the key biological processes.

BiNGO and MiMI are valuable analysis tools that are integrated into the Cytoscape framework. The GO networks created by BiNGO identify the statistically overrepresented ontologies associated with a given gene or protein dataset. This enables rapid identification and characterization of ontologies (biological process, molecular function, cellular location) that are specific to a given dataset, as well as the hierarchical nature of the ontologies. MiMI, on the other hand, gathers interaction information from various public databases and constructs an interaction network based on a list of proteins of interest. In these interaction networks, lines drawn between entities (proteins) can represent a variety of interactions, such as binding, phosphorylation, or other biologically relevant modifications. Such analyses allow for the identification of intermediary proteins that are important to the network, but are not directly identified by either biochemical analysis or literature mining. Importantly, interaction networks can be used to identify highly integrated 'hubs', which are likely to represent key factors in a given biological process or pathology.

Cell death can occur either in an unregulated or a regulated manner. Apoptosis is a well-studied regulated cell death mechanism, and awareness of regulated necrosis (necroptosis) has been increasing (Ankarcrona et al. 1995, Baines 2010, Hitomi et al. 2008). Additionally, autophagy and ER associated degradation (ERAD) are regulated processes that are vital to cell fate decisions during injurious conditions (Liu et al. 2010, Petrovski et al. 2011). Importantly, Liu et al. (2010) recently reported that cerebral ischemia induces protein aggregation, leading to multiple organelle damage that is likely to be responsible for delayed neuronal death. We constructed an IS protein interaction network that enabled the identification of five proteins that appear to be critical in linking the consequences of synaptic ischemia to regulated cell death processes (**Fig. 9**). Of the proteins identified, Vim appeared to provide the strongest association with apoptosis, whereas Hsp90aa1 was the protein that provided a link to necroptosis and ERAD. Although Vim is an intermediate filament protein expressed in glia that may not be expected to be found in the synapse, it is common to find proteins such as Vim and Gfap in synaptosomal preparations (Costain et al. 2008) and is likely to be due to the intimate association between glia and synaptic structures. Nonetheless, up-regulation of Vim following cerebral ischemia has been frequently reported, and is thought to represent the activation of astrocytes and the reactive gliosis process. Furthermore, genetic ablation of Vim has been shown to counteract neuronal pathology, indicating that Vim is relevant to ischemic synaptosomal function (Pekny & Pekna 2004). Similarly, up-regulation of heat shock proteins, such as Hsp27 and Hsp70, in response to cerebral ischemia is a well-documented finding (Franklin et al. 2005, Currie & Plumier 1998). The Hsp90 family of molecular chaperones are involved in a variety of cellular processes, such as signal transduction, protein folding and protein degradation. Hsp90aa1 is the inducible cytoplasmic form of Hsp90 and aids in the folding of a wide variety of proteins. While other ischemia-responsive heat shock proteins that are associated with MCAO were identified in the present study (**Table 1** and **2**; Hspd1, Hspa9), Hsp90aa1 has not previously been associated with cerebral ischemia and is therefore a good candidate for further examination of its role in ischemia-induced necroptosis and ERAD.

The IS network analysis indicated that autophagy was associated with the IS dataset though the cytoskeletal protein Tuba4a (**Fig. 9**). Tuba4a has previously been identified as a synaptic protein, but has not been associated with MCAO. Alterations in cellular cytoskeletal proteins, such as Map2, are known to occur following exposure to ischemic injury (Kharlamov et al. 2009) and the observed reduction in Tuba4a expression is consistent with disruption of cytoskeletal structures. Reduced expression in other tubulin/tubulin related

proteins (Tubb4, Tubb5, Tppp) was also observed, indicating an autophagy-mediated failure in the microtubule system and collapse of the synaptic structure function relationship.
Another interesting finding to arise from the IS network analysis is the prominence of the transcription factor Taf1 in connecting the autophagy, ERAD and necroptosis sub-networks. While Taf1 is involved in basal transcription, it has recently been found to be an important factor in certain neurodegenerative conditions (Davidson et al. 2009, Sako et al. 2011). Similarly, the down-regulated protein Ywhag was a highly integrated protein within the IS network, whereas the related protein Ywhaq was up-regulated with fewer interconnections (**Fig. 9**). There is growing interest in Ywhag as a mediator of neuroprotection in cerebral ischemia (Dong et al. 2010) and the observed decrease in its expression is consistent with the activation of cell death pathways. Additionally, up-regulation of Ywhaq has been observed in amyotrophic lateral sclerosis patients (Malaspina et al. 2000), and has been found to be necessary for autophagy (Wang et al. 2010). These findings suggest that the 14-3-3 proteins are likely to be playing an important role in mediating post-ischemic neuronal cell death and are good targets for therapeutic intervention in stroke.
The role of mitochondria in the pathology of ischemic neuronal death (apoptotic and necrotic) is well established (Iijima 2006, Tsujimoto & Shimizu 2007). Cerebral ischemia results in a sustained increase in intracellular Ca^{++} that is buffered by the mitochondria. The increased Ca^{++} levels disrupt the mitochondrial membrane potential and induce the formation of the permeability transition pore, thereby activating the intrinsic apoptosis pathway (Tsujimoto & Shimizu 2007). In the synaptosome, hypoxia induces mitochondrial membrane potential disruption (Aldinucci et al. 2007) and Brown *et al* (2006) have demonstrated that synaptic mitochondria are more sensitive to Ca^{++} overload than non-synaptic mitochondria. Our present findings confirm our previous observation that widespread alterations in protein expression occur in post-ischemic synaptic mitochondria (Costain et al. 2010). An interaction network was constructed from the large number of IS proteins that are involved in oxidative phosphorylation (**Fig. 10**). This interaction network clearly demonstrates that cerebral ischemia induces an imbalance in oxidative phosphorylation, with down-regulation of complex IV components and more variable effects on complex I and V. While oxidative phosphorylation is clearly disrupted, there is evidence that the cells are attempting to compensate by up-regulating glycolytic enzymes (**Fig. 11A**) as well as proteins with anti-oxidative activity (**Fig. 11B**). Unfortunately, glycolysis cannot produce the same amount of ATP that is derived from oxidative phosphorylation.
A wide variety of protein kinases are involved in mediating regulated cell death, and we identified a subset of 24 protein kinases within the IS dataset. An interaction network was constructed from the IS kinases subset (**Fig. 12**) and the kinase network independently identified three of the key proteins singled out in the IS network analysis (**Fig. 9**), supporting the contention that these proteins are involved in post-ischemic cell signaling pathways. Hsp90aa1, Taf1 and Vim were essential for connecting the four cell death mechanisms to the IS dataset, and their association with alterations in protein kinase levels further confirms their importance in mediating synaptic pathology.

5. Conclusion

In closing, this study has demonstrated that the synapse is highly responsive to cerebral ischemia and is highly informative about cerebral ischemia-induced cell death mechanisms at the organelle level. We have used interaction network analyses of the IS dataset to clarify

the effects cerebral ischemia on metabolic function, as well as to identify five proteins that are integral to cell death pathways and are potential targets for therapeutic intervention. This report also confirms that cerebral ischemia induces marked aberrations in synaptic mitochondria, lysosomes, endoplasmic reticulum and golgi apparatus, thereby emphasizing the interplay between organelles during oxidative damage.

6. References

Abe, K., Chisaka, O., Van Roy, F. & Takeichi, M. (2004) Stability of dendritic spines and synaptic contacts is controlled by alpha N-catenin. *Nature Neuroscience,* 7, 357-363.

Aldinucci, C., Carretta, A., Ciccoli, L., Leoncini, S., Signorini, C., Buonocore, G. & Pessina, G. P. (2007) Hypoxia affects the physiological behavior of rat cortical synaptosomes. *Free Radical Biology and Medicine,* 42, 1749-1756.

Ankarcrona, M., Dypbukt, J. M., Bonfoco, E., Zhivotovsky, B., Orrenius, S., Lipton, S. A. & Nicotera, P. (1995) Glutamate-induced neuronal death: a succession of necrosis or apoptosis depending on mitochondrial function. *Neuron,* 15, 961-973.

Baines, C. P. (2010) Role of the mitochondrion in programmed necrosis. *Front Physiol,* 1, 156.

Brown, M. R., Sullivan, P. G. & Geddes, J. W. (2006) Synaptic mitochondria are more susceptible to Ca2+overload than nonsynaptic mitochondria. *Journal of Biological Chemistry,* 281, 11658-11668.

Chen, X., Karnovsky, A., Sans, M. D., Andrews, P. C. & Williams, J. A. (2010) Molecular characterization of the endoplasmic reticulum: insights from proteomic studies. *Proteomics,* 10, 4040-4052.

Cheng, D., Hoogenraad, C. C., Rush, J. et al. (2006) Relative and absolute quantification of postsynaptic density proteome isolated from rat forebrain and cerebellum. *Molecular and Cellular Proteomics,* 5, 1158-1170.

Costain, W. J., Haqqani, A. S., Rasquinha, I., Giguere, M. S., Slinn, J., Zurakowski, B. & Stanimirovic, D. B. (2010) Proteomic analysis of synaptosomal protein expression reveals that cerebral ischemia alters lysosomal Psap processing. *Proteomics,* 10, 3272-3291.

Costain, W. J., Rasquinha, I., Sandhu, J. K., Rippstein, P., Zurakowski, B., Slinn, J., Macmanus, J. P. & Stanimirovic, D. B. (2008) Cerebral ischemia causes dysregulation of synaptic adhesion in mouse synaptosomes. *Journal of Cerebral Blood Flow and Metabolism,* 28, 99-110.

Couchman, J. R. (2003) Syndecans: proteoglycan regulators of cell-surface microdomains? *Nature Reviews Molecular Cell Biology,* 4, 926-937.

Currie, R. W. & Plumier, J. C. (1998) The heat shock response and tissue protection. In: *Delayed preconditioning and adaptive cardioprotection*, (G. F. Baxter and D. M. Yellon eds.), Vol. 207, pp. 135-153. Kluwer Academic Publishers, Dordrecht ; Boston.

Davidson, M. E., Kerepesi, L. A., Soto, A. & Chan, V. T. (2009) D-Serine exposure resulted in gene expression changes implicated in neurodegenerative disorders and neuronal dysfunction in male Fischer 344 rats. *Archives of Toxicology,* 83, 747-762.

DeGracia, D. J., Kumar, R., Owen, C. R., Krause, G. S. & White, B. C. (2002) Molecular pathways of protein synthesis inhibition during brain reperfusion: implications for neuronal survival or death. *Journal of Cerebral Blood Flow and Metabolism,* 22, 127-141.

Deisseroth, K., Mermelstein, P. G., Xia, H. & Tsien, R. W. (2003) Signaling from synapse to nucleus: the logic behind the mechanisms. *Current Opinion in Neurobiology,* 13, 354-365.

Dong, Y., Zhao, R., Chen, X. Q. & Yu, A. C. (2010) 14-3-3gamma and neuroglobin are new intrinsic protective factors for cerebral ischemia. *Molecular Neurobiology,* 41, 218-231.

Ehlers, M. D. (2002) Molecular morphogens for dendritic spines. *Trends in Neurosciences,* 25, 64-67.

Enright, L. E., Zhang, S. & Murphy, T. H. (2007) Fine mapping of the spatial relationship between acute ischemia and dendritic structure indicates selective vulnerability of layer V neuron dendritic tufts within single neurons in vivo. *Journal of Cerebral Blood Flow and Metabolism,* 27, 1185-1200.

Franklin, T. B., Krueger-Naug, A. M., Clarke, D. B., Arrigo, A. P. & Currie, R. W. (2005) The role of heat shock proteins Hsp70 and Hsp27 in cellular protection of the central nervous system. *International Journal of Hyperthermia,* 21, 379-392.

Gasic, G. P. & Nicotera, P. (2003) To die or to sleep, perhaps to dream. *Toxicology Letters,* 139, 221-227.

Ge, P., Luo, Y., Liu, C. L. & Hu, B. (2007) Protein aggregation and proteasome dysfunction after brain ischemia. *Stroke,* 38, 3230-3236.

Gilbert, R. W., Costain, W. J., Blanchard, M. E., Mullen, K. L., Currie, R. W. & Robertson, H. A. (2003) DNA microarray analysis of hippocampal gene expression measured twelve hours after hypoxia-ischemia in the mouse. *Journal of Cerebral Blood Flow and Metabolism,* 23, 1195-1211.

Ginsberg, M. D. (2008) Neuroprotection for ischemic stroke: past, present and future. *Neuropharmacology,* 55, 363-389.

Haqqani, A. S., Kelly, J. F. & Stanimirovic, D. B. (2008) Quantitative protein profiling by mass spectrometry using label-free proteomics. *Methods in Molecular Biology,* 439, 241-256.

Hasbani, M. J., Schlief, M. L., Fisher, D. A. & Goldberg, M. P. (2001) Dendritic spines lost during glutamate receptor activation reemerge at original sites of synaptic contact. *Journal of Neuroscience,* 21, 2393-2403.

Havik, B., Rokke, H., Bardsen, K., Davanger, S. & Bramham, C. R. (2003) Bursts of high-frequency stimulation trigger rapid delivery of pre-existing alpha-CaMKII mRNA to synapses: a mechanism in dendritic protein synthesis during long-term potentiation in adult awake rats. *European Journal of Neuroscience,* 17, 2679-2689.

Hirosawa, M., Hoshida, M., Ishikawa, M. & Toya, T. (1993) MASCOT: multiple alignment system for protein sequences based on three-way dynamic programming. *Computer Applications in the Biosciences,* 9, 161-167.

Hitomi, J., Christofferson, D. E., Ng, A., Yao, J., Degterev, A., Xavier, R. J. & Yuan, J. (2008) Identification of a molecular signaling network that regulates a cellular necrotic cell death pathway. *Cell,* 135, 1311-1323.

Hou, S. T. & MacManus, J. P. (2002) Molecular mechanisms of cerebral ischemia-induced neuronal death. *International Review of Cytology,* 221, 93-148.

Iijima, T. (2006) Mitochondrial membrane potential and ischemic neuronal death. *Neuroscience Research,* 55, 234-243.

Jordan, B. A., Fernholz, B. D., Boussac, M., Xu, C., Grigorean, G., Ziff, E. B. & Neubert, T. A. (2004) Identification and verification of novel rodent postsynaptic density proteins. *Molecular and Cellular Proteomics,* 3, 857-871.

Kagedal, K., Johansson, U. & Ollinger, K. (2001) The lysosomal protease cathepsin D mediates apoptosis induced by oxidative stress. *FASEB Journal,* 15, 1592-1594.

Kharlamov, A., LaVerde, G. C., Nemoto, E. M., Jungreis, C. A., Yushmanov, V. E., Jones, S. C. & Boada, F. E. (2009) MAP2 immunostaining in thick sections for early ischemic stroke infarct volume in non-human primate brain. *Journal of Neuroscience Methods,* 182, 205-210.

Li, K. W., Hornshaw, M. P., Van Der Schors, R. C. et al. (2004) Proteomics analysis of rat brain postsynaptic density. Implications of the diverse protein functional groups for the integration of synaptic physiology. *Journal of Biological Chemistry,* 279, 987-1002.

Liu, C., Gao, Y., Barrett, J. & Hu, B. (2010) Autophagy and protein aggregation after brain ischemia. *Journal of Neurochemistry,* 115, 68-78.

MacManus, J. P., Graber, T., Luebbert, C., Preston, E., Rasquinha, I., Smith, B. & Webster, J. (2004) Translation-state analysis of gene expression in mouse brain after focal ischemia. *Journal of Cerebral Blood Flow and Metabolism,* 24, 657-667.

Malaspina, A., Kaushik, N. & de Belleroche, J. (2000) A 14-3-3 mRNA is up-regulated in amyotrophic lateral sclerosis spinal cord. *Journal of Neurochemistry,* 75, 2511-2520.

Martone, M. E., Jones, Y. Z., Young, S. J., Ellisman, M. H., Zivin, J. A. & Hu, B. R. (1999) Modification of postsynaptic densities after transient cerebral ischemia: a quantitative and three-dimensional ultrastructural study. *Journal of Neuroscience,* 19, 1988-1997.

Mattson, M. P. & Duan, W. (1999) "Apoptotic" biochemical cascades in synaptic compartments: roles in adaptive plasticity and neurodegenerative disorders. *Journal of Neuroscience Research,* 58, 152-166.

Mattson, M. P. & Gleichmann, M. (2005) The neuronal death protein par-4 mediates dopaminergic synaptic plasticity. *Molecular Interventions,* 5, 278-281.

Mattson, M. P., Keller, J. N. & Begley, J. G. (1998) Evidence for synaptic apoptosis. *Experimental Neurology,* 153, 35-48.

Morciano, M., Burre, J., Corvey, C., Karas, M., Zimmermann, H. & Volknandt, W. (2005) Immunoisolation of two synaptic vesicle pools from synaptosomes: a proteomics analysis. *Journal of Neurochemistry,* 95, 1732-1745.

Park, J. S., Bateman, M. C. & Goldberg, M. P. (1996) Rapid alterations in dendrite morphology during sublethal hypoxia or glutamate receptor activation. *Neurobiology of Disease,* 3, 215-227.

Passafaro, M., Nakagawa, T., Sala, C. & Sheng, M. (2003) Induction of dendritic spines by an extracellular domain of AMPA receptor subunit GluR2. *Nature,* 424, 677-681.

Pastuszko, A., Wilson, D. F. & Erecinska, M. (1982) Neurotransmitter metabolism in rat brain synaptosomes: effect of anoxia and pH. *Journal of Neurochemistry,* 38, 1657-1667.

Pedrioli, P. G., Eng, J. K., Hubley, R. et al. (2004) A common open representation of mass spectrometry data and its application to proteomics research. *Nature Biotechnology,* 22, 1459-1466.

Pekny, M. & Pekna, M. (2004) Astrocyte intermediate filaments in CNS pathologies and regeneration. *Journal of Pathology,* 204, 428-437.

Peng, J., Elias, J. E., Thoreen, C. C., Licklider, L. J. & Gygi, S. P. (2003) Evaluation of multidimensional chromatography coupled with tandem mass spectrometry (LC/LC-MS/MS) for large-scale protein analysis: the yeast proteome. *Journal of Proteome Research,* 2, 43-50.

Peng, J., Kim, M. J., Cheng, D., Duong, D. M., Gygi, S. P. & Sheng, M. (2004) Semiquantitative proteomic analysis of rat forebrain postsynaptic density fractions by mass spectrometry. *Journal of Biological Chemistry,* 279, 21003-21011.

Petrovski, G., Das, S., Juhasz, B., Kertesz, A., Tosaki, A. & Das, D. K. (2011) Cardioprotection by endoplasmic reticulum stress-induced autophagy. *Antioxidants & Redox Signaling,* 14, 2191-2200.

Phillips, G. R., Florens, L., Tanaka, H., Khaing, Z. Z., Fidler, L., Yates, J. R., 3rd & Colman, D. R. (2005) Proteomic comparison of two fractions derived from the transsynaptic scaffold. *Journal of Neuroscience Research,* 81, 762-775.

Rafalowska, U., Erecinska, M. & Wilson, D. F. (1980) The effect of acute hypoxia on synaptosomes from rat brain. *Journal of Neurochemistry,* 34, 1160-1165.

Sako, W., Morigaki, R., Kaji, R., Tooyama, I., Okita, S., Kitazato, K., Nagahiro, S., Graybiel, A. M. & Goto, S. (2011) Identification and localization of a neuron-specific isoform of TAF1 in rat brain: implications for neuropathology of DYT3 dystonia. *Neuroscience,* 189, 100-107.

Schrimpf, S. P., Meskenaite, V., Brunner, E., Rutishauser, D., Walther, P., Eng, J., Aebersold, R. & Sonderegger, P. (2005) Proteomic analysis of synaptosomes using isotope-coded affinity tags and mass spectrometry. *Proteomics,* 5, 2531-2541.

Stevens, S. M., Jr., Zharikova, A. D. & Prokai, L. (2003) Proteomic analysis of the synaptic plasma membrane fraction isolated from rat forebrain. *Brain Research. Molecular Brain Research,* 117, 116-128.

Sulkowski, G., Waskiewicz, J., Walski, M., Januszewski, S. & Rafalowska, U. (2002) Synaptosomal susceptibility on global ischaemia caused by cardiac arrest correlated with early and late times after recirculation in rats. *Resuscitation,* 52, 203-213.

Taylor, S. W., Fahy, E., Zhang, B. et al. (2003) Characterization of the human heart mitochondrial proteome. *Nature Biotechnology,* 21, 281-286.

Tsujimoto, Y. & Shimizu, S. (2007) Role of the mitochondrial membrane permeability transition in cell death. *Apoptosis,* 12, 835-840.

Vanderklish, P. W. & Bahr, B. A. (2000) The pathogenic activation of calpain: a marker and mediator of cellular toxicity and disease states. *International Journal of Experimental Pathology,* 81, 323-339.

Wang, B., Ling, S. & Lin, W. C. (2010) 14-3-3Tau regulates Beclin 1 and is required for autophagy. *PLoS ONE,* 5, e10409.

Witzmann, F. A., Arnold, R. J., Bai, F. et al. (2005) A proteomic survey of rat cerebral cortical synaptosomes. *Proteomics,* 5, 2177-2201.

Yamashima, T. & Oikawa, S. (2009) The role of lysosomal rupture in neuronal death. *Progress in Neurobiology,* 89, 343-358.

Zhang, S. & Murphy, T. H. (2007) Imaging the impact of cortical microcirculation on synaptic structure and sensory-evoked hemodynamic responses in vivo. *PLoS Biology,* 5, e119.

Zhao, H., Shimohata, T., Wang, J. Q., Sun, G., Schaal, D. W., Sapolsky, R. M. & Steinberg, G. K. (2005) Akt contributes to neuroprotection by hypothermia against cerebral ischemia in rats. *Journal of Neuroscience,* 25, 9794-9806.

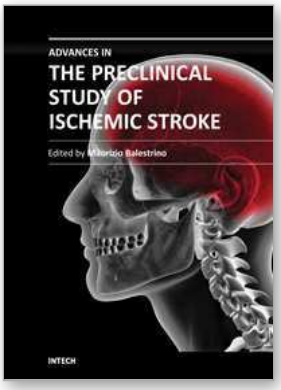

Advances in the Preclinical Study of Ischemic Stroke
Edited by Dr. Maurizio Balestrino

ISBN 978-953-51-0290-8
Hard cover, 530 pages
Publisher InTech
Published online 16, March, 2012
Published in print edition March, 2012

This book reports innovations in the preclinical study of stroke, including - novel tools and findings in animal models of stroke, - novel biochemical mechanisms through which ischemic damage may be both generated and limited, - novel pathways to neuroprotection. Although hypothermia has been so far the sole "neuroprotection" treatment that has survived the translation from preclinical to clinical studies, progress in both preclinical studies and in the design of clinical trials will hopefully provide more and better treatments for ischemic stroke. This book aims at providing the preclinical scientist with innovative knowledge and tools to investigate novel mechanisms of, and treatments for, ischemic brain damage.

INTECH
open science | open minds

InTech Europe
University Campus STeP Ri
Slavka Krautzeka 83/A
51000 Rijeka, Croatia
Phone: +385 (51) 770 447
Fax: +385 (51) 686 166
www.intechopen.com

InTech China
Unit 405, Office Block, Hotel Equatorial Shanghai
No.65, Yan An Road (West), Shanghai, 200040, China
中国上海市延安西路65号上海国际贵都大饭店办公楼405单元
Phone: +86-21-62489820
Fax: +86-21-62489821